Low Frequency Study of Rotating Radio Transients

Michael McCrackan

Dr. Kevin Stovall

Dr. Gregory Taylor

Abstract

Rotating Radio Transients are a recently discovered type of radio emitting pulsar that, while possessing similar pulse widths and pulse intensities to those of the 2000 other regular pulsars that have been discovered thus far, differ from those due to their exhibiting a variability in the emission of their individual pulses. The pulses of RRATs are only observed intermittently, and individual pulses are found to be detected on timescales ranging from a few seconds up to a few hours apart. As the reason for this differing behavior of RRATs is still unsolved, RRATs may potentially play an important role in in our understanding of the emission mechanism of pulsars and the supernova rate of our galaxy. Utilizing the first station of the Long Wavelength Array Telescope, 18 RRATs were observed at frequencies less than 100 MHz, representing a region of the electromagnetic spectrum where these pulsars have had no significant prior studies. Of the 18 observed, 3 detections were made and several properties of these RRATs were determined.

Introduction

It was the detection of a periodic signal in 1967 from an astrophysical source that pulsed with never before observed consistency and on previously unseen short timescales that revealed to the world the existence of neutron stars or more specifically, the subclass that soon came to be known as pulsars. These exotic objects, whose existence was theorized some 30 years before their actual discovery, have secured a considerable interest from the scientific community since their discovery, due in part to their many unusual and curious properties, and their ability to contribute to the advancement of a number of other fields of astrophysics. They contribute to the fields of stellar, nuclear and condensed matter physics, studies of the interstellar medium through the scattering of the radio emissions from pulsars, and in research concerning gravitational waves through pulsar timing arrays and observations of neutron star binary systems. Indeed, it was the 1993 discovery of the decrease in the orbital period of a binary neutron star system that provided the first indirect, yet crucial, evidence for the existence of the gravitational waves predicted by Einstein many years earlier [14, 40, 46, 61].

Adding to the many interesting properties that separate them from other phenomena in the universe, studies of neutron stars at radio, optical, x-ray, and gamma ray wavelengths have also exposed a considerable amount of diversity to exist amongst neutron stars themselves. Neutron stars vary in mass, rotational periods, magnetic field strengths, temperatures, and more. There are neutron stars with periods of only a few milliseconds and those with periods of more than a few seconds, those neutron stars, now referred to as magnetars, which possess magnetic fields far higher than those of most of the other neutron stars observed so far, neutron stars in binary systems with both other neutron stars and other objects. There are those with planetary sized bodies orbiting around them, and even neutron stars with large peculiar velocities and no longer reside in the area in which they originally formed. Each of

these cases provides insight not only into the structure of neutron stars, but also offer clues about the conditions under which they form, how they evolve with time, and about the final stages of the stars that produce them [14, 46].

Continuing this trend of diversity, the category of neutron stars that emit beams of radiation which cross our line of sight producing an on/off or "lighthouse effect," or pulsars, also exhibit a great deal of non-uniformity. The emitted pulses from these objects differ from one another in their pulse intensities, widths, and shapes, and the pulses of an individual pulsar can change from one pulse to the next. Many pulsars, such as the infamous Crab Pulsar, spontaneously emit giant pulses that can be brighter than their regularly emitted pulses by several thousand times, and there are pulsars that exhibit drifting sub-pulses with distinct shapes and at different periods than those of the main pulse. While the rotation rate of pulsars are observed to slow down with time, albeit very slowly, there are those pulsars that undergo "glitches" or sudden speed ups, which are thought to be the result of the elastic nature within the neutron star's interior. There are also pulsars that undergo phases where they either emit very weakly, as in the case of many X-ray isolated neutron stars, or those that cease their emission entirely for timescales ranging from only a few seconds to several weeks, before suddenly starting up their pulsations again on similar timescales. The latter of these are referred to as nulling pulsars and the origin of this nulling phenomena, which can range from a few percent up to 95 percent of the observing time, is a topic of intense study. Indeed, the emission mechanism and the numerous other properties of pulsars altogether, has yet to be fully explained, although a considerable number of theories have been developed that take into account various neutron star composition models and other effects [14, 46].

In 2006, this already complex zoology of neutron stars received a new addition in the form of a pulsar that demonstrated an extreme degree of variability which had not been observed in pulsars previously. Now referred to as Rotating Radio Transients, illustrating their initial discovery at radio frequencies, these pulsars only emit single pulses that are separated in time from each other by seconds, minutes, or hours depending on the particular RRAT. This transient nature differs from the aforementioned pulsing phenomena of nulling pulsars, in that nulling pulsars emit several pulses at a time, before turning off for some time, whereas RRATs only emit single pulses; this property largely prevents RRATs from being detected in the more often utilized searches for periodic signals, thereby explaining their lack of being discovered until a few years ago [24, 51].

Currently, nearly 100 RRATs have been identified in a number of sky surveys at radio frequencies, and their transient emissions have not yet received a thorough explanation. There is some observational evidence for RRATs potentially being older pulsars that are near the point of "switching off" or that they may be similar to nulling or middle aged pulsars known as X-ray isolated neutron stars. The differing pulsing nature might not even be due to the neutron star itself, but might be a byproduct of a debris field orbiting the neutron star, consequently preventing our detection of the emitted beam. The unravelling of the phenomena behind the single pulse variability of these neutron stars is a necessary task, as statistical studies based upon the number of RRATs found in the initial survey that first found them reveals that there may be substantially more RRATs than regular pulsars in the galaxy. This may have profound consequences on the currently accepted supernova rate of the galaxy, as the current accepted value for the supernova rate in the galaxy may be insufficient to account for the existence of RRATs should these transient pulsars prove to be a population that is completely distinct from regular and nulling pulsars. This makes a more detailed understanding of their properties and emission mechanism a crucial component in the understanding of neutron stars and supernovae in our galaxy [24, 51, 70].

Here, we present the preliminary results of a study of Rotating Radio Transients with the Long Wavelength Array at frequencies below 100 MHz. The long wavelength universe is one of the least studied regions of the electromagnetic spectrum and no large studies of RRATs have been carried out at these wavelengths to date. The LWA is a powerful instrument for studies of a variety of astrophysical phenomena at these frequencies, having proven itself able to detect a number regular pulsars and place more precise constraints on many of their properties, as a result of its high time and frequency resolution. For this reason, 18 RRATs with dispersion measures less than 100 pc cm^{-3} that were previously identified in single pulse searches by other radio observatories at higher frequencies were observed with the LWA. The goal of these observations was to determine the properties of this subclass of neutron stars at long wavelengths, potentially ascertaining whether their spectral properties would make them easier to observe there and whether or not their pulse profiles differed when compared to the higher frequency observations. Of the 18 RRATs that were observed with the LWA, only 3 were detected. From these detections, a number of the aforementioned properties were determined and for those that were not detected, several constraints can be placed on the properties of RRATs at low frequencies, which may depend on the number of emitted pulses for a given amount of time, the flux densities of the individual pulses, and the sensitivity of the LWA.

A Review of Neutron Stars

Understanding the properties and structure of neutron stars characterizes a key step forward in furthering the understanding of the mechanisms that result in the emission of the radio beams from pulsars and the unusual pulsing nature of RRATs. The theories predicting the existence of neutron stars were well in place long before the first observational evidence of their existence was found in the form of the detection of an apparently periodic series of pulses. Walter Baade and Fritz Zwicky in 1934 considered the possibility that the cores of supermassive stars (those with masses larger than 8 to 10 solar masses) could undergo a radical transformation upon the end of the nuclear fusion processes within their inner layers that dominate most of the star's life [2, 3]. Following the repeated fusion, expansion, collapse, and re-ignition of fusion of subsequently heavier and heavier elements within the core that eventually ends with a core composed primarily of Iron nuclei, the inability of any further fusion to provide a resisting pressure to the inwards pull of gravity causes a final collapse in the stellar core. With its large mass, the core's collapse dramatically increases the temperature to the point where the photons have sufficient energy to "photodisintegrate" the nuclei there, breaking them down into individual neutrons, protons, and electrons [14, 41].

The collapse continues and the electron degeneracy pressure, or the force due to the electrons being fermions and not wanting to occupy the same state as other electrons – this force is responsible for preventing the gravitational collapse of the already dense white dwarf stars in our universe – is overcome and the electrons then combine with the protons to form neutrons. This combination reaction releases a prodigious number of neutrinos that carry away vast amounts of energy, speeding the collapse until the point where the neutron degeneracy pressure kicks in when the density attains a value near that of nuclear density. The collapse is finally terminated and the outer layers of the star that are still composed of regular nuclei are then blown off due to the rebound from this sudden stop in an explosive supernova event, leaving behind the resulting neutron star [14, 41].

Despite the early predictions about their existence, neutron stars are still poorly understood objects, partly due to the difficulty in observing these small, dense stars directly. Whereas regular stars reveal

their inner processes through the photons released by their interior nuclear fusion processes, neutron stars are rarely detected directly if not for pulsars, or in some cases through their X-ray thermal emissions. Models of the progenitor star's interior, other physical constraints, such as an approximate upper bound on the mass of neutron stars, and observational studies of their temperatures, rotation rates, magnetic fields, and more all contribute to constraining their properties. The general predicted structure of neutron stars is given by the Tolman-Oppenheimer-Volkov (TOV) equations that relate the pressure and mass to the radial distance from the center of the star; solutions of the TOV equation provide equations of state or mathematical relations between the density and pressure. From these, it is theorized that neutron stars possess several layers of differing compositions, which include the inner and outer cores, the crust, an envelope surrounding the crust, and an atmosphere. The properties of the outer layers are fairly well-constrained, as the matter there is not expected to have transformed into the more exotic forms of matter that are hypothesized to exist in the deeper layers [14, 26, 41].

The crust of a neutron star is a thin 1-2 km layer at the surface and is primarily composed of neutron rich nuclei, such as 56 Fe, with a density that is less than that of nuclear density. With increasing depth, the nuclei become more neutron enriched and distorted into various lattice arrangements, known as nuclear pasta, until their neutron excesses reach the "neutron drip line," where it becomes more energetically favorable for neutrons to exist outside of nuclei. The remaining protons and electrons largely combine with one another to form neutrons, as was the case during the initial collapse in the core during the supernova. This results in a neutron superfluid in the outer core that can couple to the crust due to its elastic nature and transfer angular momentum to it, producing the observable neutron star glitches or sudden increases in the rotation rate of the neutron star. In the deepest part of the star, the inner core, the composition is currently unknown, with the potential for unconfined quark superfluids, pions, kaons, and/or hyperonic matter. Together, the inner and outer cores comprise nearly 90-99% of the neutron star's mass [14, 26, 41].

Finally, the atmosphere makes up the outermost layer of the neutron star and contributes the least mass, being only a few meters thick. It is thought to be primarily composed of both light and heavy nuclei, with the former being left over debris from the supernova and the latter rising from accretion processes. It is generally expected to be optically thick and there have been detections for a variety of absorption lines in many isolated neutron star thermal blackbody spectra, with models pointing to these likely resulting from hydrogen and perhaps helium or other heavier elements. Observations and theories indicate that these atmospheres exist in a highly magnetized field that exists due to the conservation of magnetic flux during the collapse of the progenitor star's core – the core already retains a considerable magnetic field, but with the sudden drop in size down to radius of a few kilometers, the magnetic flux must therefore increase by the same factor as the decrease in the surface area. This dipole field, which has a field strength oftentimes in excess of 10^{10} G, or even 10^{13} G to 10^{15} G for some special neutron stars, causes the radiation to propagate in two polarizations and forces the free electrons and positrons that exist in a neutral plasma to move along the field lines; these play an important role in the emission of radiation in narrow beams from pulsars [14, 37, 41, 38, 63, 69].

A Review of Pulsars

Utilizing an array of 2048 radio dipoles at the Mullard Radio Astronomy Observatory, which was originally constructed to carry out observations of the scintillation of radio waves at a frequency of 81.5 MHz from such distant objects as quasars, Joceyln Bell and Antony Hewish became the first to detect a signal from

a pulsar in July 1967. Due to the fact that the signal reappeared every sidereal day, Bell correctly concluded that this detection did not originate from the Earth, but was of astrophysical origin, and more detailed inspections revealed that the pulses were actually emitted more frequently, being separated in time from one another by 1.337 seconds. A pulsation of this precision and short time scale had not been observed previously, leading some to offer that this signal may have been of intelligent extraterrestrial origin, but this was quickly rendered exceedingly unlikely due to the discovery of a second such signal a year later and even more in the next few years by separate radio observatories [14, 46].

in 1966 it was suggested that neutron stars may be able to provide energy to the surrounding supernova remnant from which they appeared, and Franco Pacini pushed this idea further in 1967, just before the first pulsar was discovered, suggesting that neutron stars may have the potential to emit radiation powered by their rotations, which could serve as the energy source to a surrounding supernova remnant and cause emission, such as in the Crab Nebula [6, 53]. Along the same lines, Thomas Gold in 1968 correctly reasoned that neutron stars were not only the origin of the observed pulses, but that these consistent pulses originated from the neutron star's rotation and not some other effect. He ruled out a number of other potential origins, including oscillations of white dwarfs or neutron stars and plasma physics effects, due to the fine structure exhibited in the pulses, the short durations of the pulses, which implies a small emitting region and a high gravitational field, and due to the fact that in stellar oscillations, the lowest oscillation mode of that star must be similar in magnitude to the period of the star. This is fairly unlikely in the case of a neutron star, as the modes would require a long period, else the star would become flattened to a significant extent [36]. Gold's views were not entirely accepted until the discovery of PSR B0531+21, the Crab Pulsar, in 1968 first by David H. Staelin and Edward C. Reifenstein III with the 100 m Green Bank Telescope and its detection was confirmed and the period measured later that year by Richard Lovelace and others utilizing the Arecibo observatory [5]. With its short 33 millisecond pulsing period, far too short to be accounted by the significantly less dense white dwarfs and other sources, there was no doubt that the origin of pulsars was from the emissions of rotating neutron stars [5, 46].

At the time of Gold's theories, the exact nature of the emission mechanism of neutron stars was not entirely understood and the primary idea was that the pulsar phenomenon may be powered either by energy from within the neutron star or from its rotational energy. In the latter case, the existence of the powerful magnetic field of the neutron star would result in a magnetosphere that partially rotates along with the neutron star and plasma in the region around the neutron star would be forced to move at relativistic velocities within the light cylinder (the region where the velocity of the particles is less than the speed of light). Should an asymmetry in the field exist, perhaps originating from the original supernova that produced the neutron star, it was reasoned that sufficiently energetic plasma could be launched from regions where the surface is non-uniform, resulting in the release of a radio beam [5].

Continued observations in the form of directed searches of supernovae remnants and blind searches, or observations of large portions of the sky that look for any detections of new pulsars, with such observatories as the Green-Banks Telescope, the Arecibo Radio Observatory, and the Effelsberg Telescope have not only revealed the presence of nearly 2000 pulsars, but have also have illustrated the large amount of diversity that defines pulsars [12, 47]. Some of the notable discoveries of pulsars include Hulse and Taylor's discovery of a binary pulsar system in an Arecibo telescope survey with an orbital period of 7.75 hours, for which later observations detected a change in orbital period signaling the emission of energy in the form of gravitational waves [65]. The Arecibo telescope was also the first to detect PSR B1937+21 in 1982, a pulsar with a weak magnetic field and the shortest known period of 1.6 milliseconds

at the time, thereby becoming the first millisecond pulsar to be discovered. This class of pulsar is thought to originate from the spinning up of a neutron star as it acquires angular momenta through the accretion of matter from a neighboring normal star [14, 55].

Radio observatories are not the only instruments that have carried out studies of pulsars, with detections in the optical, X-ray, and gamma ray regions of the spectra. The much studied Crab and Vela pulsars are such examples, with both having been detected at optical wavelengths and pulse in the visible similarly to how they do in the radio [6, 57]. Neutron stars that are accreting from another star in a binary system (X-ray binary systems) and the thermal emissions of many neutron stars are observable at X-ray wavelengths. In the X-ray binary case, a neutron star accretes matter when its companion star overfills its Roche Lobes and the resulting infalling of matter releases the large amounts of gravitational potential energy. Such systems are also found to produce large radio jets in addition to their X-ray emissions and can be likened to quasars. Finally, in March 5th 1979, the Soviet space probes Venera I and II, as well as NASA's Helios 2 probe, detected the strongest burst of gamma rays (over 200,000 counts per second compared to a background of approximately 100 counts per second) ever observed from an event outside of the solar system. [27]

This less than a second burst was followed by a "softer" burst that lasted several minutes, with the process being observed to repeat itself at least 16 times for a number of years and adding up to about 100 bursts in a decade. With the detection by multiple instruments, the source's location was established to be in the general direction the supernova remnant SNR 0525-66.1, identifying it as likely being a special type of neutron star. This theory was solidified when Chryssa Kouvelioto measured an increase in the pulsar's period following the bursts, corresponding to an overall decrease in energy of the neutron star, resulting from it being carried away by the burst, which was predicted to occur. This neutron star type came to be known as a soft gamma ray repeater, or a highly magnetized neutron star whose emission mechanisms likely differ considerably from those of the standard rotation powered pulsar [13, 14, 27].

Pulsar Emission Mechanisms

As with the internal structure and atmospheric models of neutron stars, the physics underlying the emission of the radio beams that define a pulsar are also not very well understood. Observations have determined that there exists a considerable disparity in the brightness temperatures of both the optical and X-ray emissions from pulsars when compared to the radio emission from pulsars, with the former being in the vicinity of 10^{11} K and the latter being as much as 10^{30} K. For the optical emission, this would correspond to fairly low energies of 10^7 eV, which can therefore be considered to be the result of incoherent emission processes. The same is not true for the radio emissions, which would require mean energies as large as 10^{26} eV. This represents such a high value that coherent emission processes are the more likely the origin of the radio photons from pulsars, for such mechanisms allow a higher flux without the need for such high particle energies. For the coherent emission processes, there exist several theories about what physical mechanisms lie behind the lighthouse beams of pulsars and they generally revolve around the pair production of electrons and protons in the neutron star's partially commoving magnetosphere [1, 14, 35, 42, 56].

The emission models involve the generation of an instability in the neutron star's surrounding plasma and they differ based upon where they expect the coherent pulsed radiation to be emitted from; the radiation might be emitted from either open field line regions or closed ones. The instabilities may arise through a variety of processes, ranging from such theories as the cyclotron instability model and the radiative

instability model to the two-stream instability model, the last of which is a plasma physics effect known to play an important role in many other astrophysical objects, including solar bursts and active galactic nuclei. In the majority of the models, the magnetic field is approximated to be an off-axis dipole magnetic field, such that the charge density of the plasma magnetosphere is related to the magnetic field strength and the angular velocity of the neutron star. The charge density can change its sign or polarity at null surface locations (see figure 1), thus producing areas that have very nearly neutral charge. This difference in charge density from its average value will create an electric field in four "outer gap" regions in the closed field models or in the polar region's "inner gaps" in the open field models. This has the result of accelerating the electron and positrons in the magnetosphere to ultra-relativistic velocities, as they travel along the magnetic field lines, thus causing them to radiate gamma rays tangent to these magnetic field [1, 16, 35, 42, 56, 62].
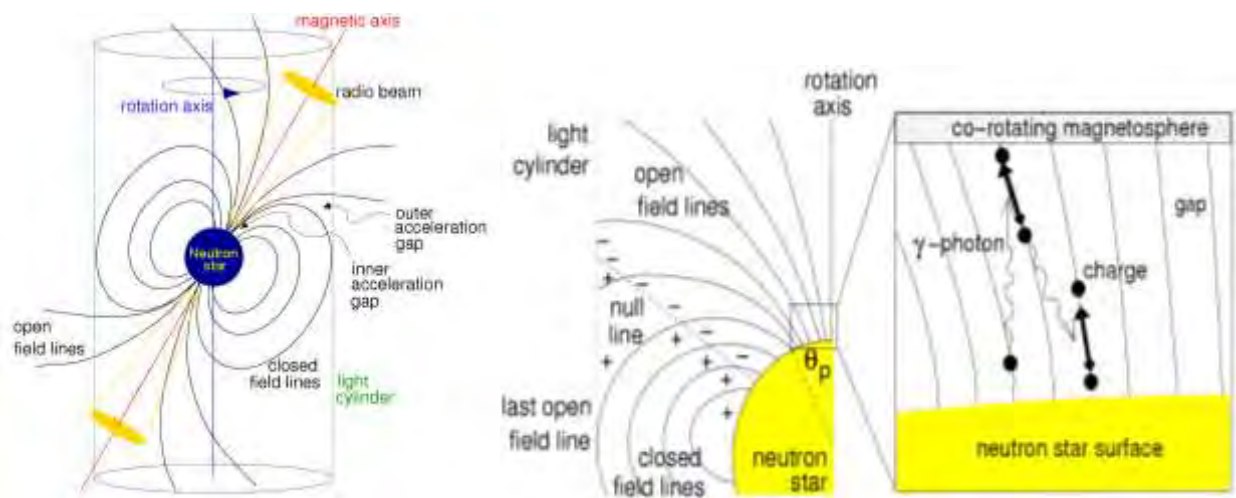

Figure (1): The general arrangement of a pulsar and its magnetosphere [18].

These electron positron pairs originate from regions near the poles of the neutron star through the process of pair production from high energy photons that are emitted from the surface of the star and make their way into the gap regions. Additionally, charged particles can be launched from the polar cap regions due to the Lorentz force acting on them by the electromagnetic fields of the magnetosphere. The photons produced from the accelerated particle pairs can also annihilate and produce more particle pairs, with electrons moving towards the surface and positrons moving outwards. The majority of these positron's kinetic energy will therefore be transformed into "curvature radiation," with the accelerated pairs producing microwave radiation and the non-accelerated ones in the outer regions producing the observed radio emissions in a dipole arrangement. The charges are thought to return along the boundaries of the outer gap region forming the high energy emissions that are seen in younger, more active pulsars [1, 16, 35, 42, 56, 62].

The returning charges can have visible effects on the surrounding gases left over from the neutron star's own supernova – they can pour energy into the supernova remnant, heating it up and ionizing it, thus causing the gas there to emit radiation. The oftentimes intense radiation pressure from the pulsar can

produce a force on the remnant, thereby creating density perturbations in the surrounding gas that can vary on timescales of hours to days, and can have a measurable effect on many of the observable qualities of the pulsar, such as the dispersion measure. The dispersion measure is not only used to determine the distances to pulsars, but also in the shapes of the individual pulses, both of which are detailed in the next section [15, 43].

Although the general pulse profile of most pulsars is essentially that of a Gaussian distribution, the properties observed in pulse's emitted from a great deal of pulsars differ not only from pulsar to pulsar, but also from pulse to pulse for the same pulsar. While there exist basic differences in pulse widths and flux densities, some pulsars, such as PSR B0329+54, exhibit additional structures, including one or more secondary peaks or even separate interpulses that can "drift" in their arrival times relative to the main pulse. This change in the difference in the arrival times between the main and sub pulses corresponds directly to difference in rotational longitude on the pulsar itself that are likely emitted from areas on the neutron star that are distinct from the polar emitting regions that produce the main pulse. These may move around on the pulsar due to plasma drifting in the magnetosphere. This drifting phenomenon is a property that is more often observed in pulsars of greater age and are hypothesized to be connected to nulling in pulsars, which is also observed more frequently in older pulsars. Such nulling pulsars as PSR B0834+06 have a distribution in their pulses that is bimodal, with probabilities existing for both a regular Gaussian pulse distribution and a nulling or no emission phase, with the potential for these nulling phases to be maintained for several pulsing periods [45, 69].

As pulsars age, they lose energy due to the constant emission of neutrinos and thermal photons from their surface, in addition to gravitational wave emissions and magnetic breaking. This results in pulsars losing angular momentum and their angular velocities slow down, an effect which can be fairly easily measured. The spin down rate is inversely proportional to their ages, decreasing as they get older, which, along with measurements of their periods, permits the ages of pulsars to be determined separately from measurements of their temperatures through X-ray detections. After sufficient time (a few million years) has passed, the periods become long enough that the potential drop across gap regions, which is dependent on the radius of curvature of the magnetic fields and the pulsar's period, becomes insufficient to ignite the required pair production and the radio emission ceases [16]. On plots of log period versus log period derivative, the region where pulsars are thought to be no longer able to emit is referred to as the pulsar death line, below which no emission is expected. An example of a p-pdot plot and the pulsar death line is illustrated later on in the discussion of RRAT emission mechanisms in figure (3).

Searching for Pulsars

There exist two primary methods of finding pulsars, referred to as single pulse searches and periodic of Fourier domain searches. The usefulness of each of these methods varies from pulsar to pulsar, based on such considerations as the strengths of their emissions, the period of the pulsar, the instrument utilized and the length of the observation with that instrument, the radio frequency interference environment, and so on [48]. The first pulsar detection by Jocelyn Bell, as well as many of the early detections immediately following it, were single pulse searches, or searches that simply look through a time series for individual bright pulses above some noise threshold. While they are still utilized today, particularly for RRAT discoveries, it was soon discovered that weak signals from pulsars with low signal to noise ratios above that of the random noise emitted from the sky and the telescope receiver system itself would be difficult to detect and identify. Therefore, instead of searching for signals in the time domain, the vast

majority of modern searches look for regular pulses carry out an investigation in the frequency domain through a Fast Fourier Transform (FFT) of the time series data. The FFT of some data containing n samples will give a power or amplitude spectrum of (n/2)+1 points with each point corresponding to a value of $\frac{k}{n\Delta t}$ (k=0, 1, 2…). If a detected signal is not a simple sinusoidal function of time, then the FFT will reveal a number of frequency elements, known as harmonics, corresponding to multiples of a single period or the fundamental frequency. The harmonic amplitudes can be summed to provide an increase in the sensitivity, particularly to narrower pulses. The sensitivity is increased by a factor of:

$$\sqrt{\frac{1-\delta}{\delta}} \qquad (1)$$

In this expression, $\delta = \frac{W}{P}$, where W is the width of the pulse (in units of time) and P is the period. Therefore, periodic searches have a higher sensitivity to longer period pulsars. Should any signal that appears to represent a pulsar candidate be found through comparison with known pulse shapes, the time series data can then be folded or overlapped with itself at a period corresponding to that found from the power spectra [33, 44, 46, 50, 54, 65].

While the numerous advantages demonstrated by FFT based searches make them preferable over the single pulse searches for regular pulsars, the detection of emissions from non-periodic pulsars, namely RRATs and giant pulse emitting pulsars, requires single pulse searches. If the signal is highly sporadic, the power spectra will not have the usual peaks associated with the fundamental frequency and its harmonics and detection will be difficult through the FFT approach. Single pulse search sensitivities depend highly on the pulse shapes, frequencies, DM errors, and bandwidths, with the signal-to-noise ratio of detections dropping for lower frequencies and rising for lower pulse widths. This SNR can be written as:

$$SNR = \frac{1}{\sigma\sqrt{W_n}}\left(\frac{A}{W}\right) \qquad (2)$$

The SNR is given as a function of the root mean squared noise σ, W_n and W, which are the correlation times or the times at which the noise and pulse are detected, and A is the intrinsic area of the pulse, given by $A = S \times W$, with S being the flux density of the pulse. This illustrates that broad pulses with less power have a greater SNR and are therefore easier to detect above the noise threshold than narrower pulses with higher power or amplitudes [17, 19].

These methods of identifying pulsar signatures, though relatively simple in their basic approaches, become more complicated due a number of effects produced by the interstellar medium that exists between us and the pulsar, as well by many of the steps that are made with the intention of correcting for these effects. As the pulse traverses through the ISM, it becomes smeared in time to an extent that is dependent on its frequency. The total time smearing is given by:

$$\Delta t = (\Delta t_{DM}^2 + \Delta t_{DM\ error}^2 + \Delta t_{\Delta v}^2 + t_d^2)^{1/2} \qquad (3)$$

Here, the first term is the time lag produced by the dispersive effects of the ISM and the second term is the error introduced in the attempts to correct for dispersion. The value of the dispersion lag is often written as:

$$\Delta t_{DM} = \frac{e^2}{2\pi c m_e}\left[\frac{1}{v_1^2} - \frac{1}{v_2^2}\right]\int_0^L N(l)dl \quad (4)$$

From this, it becomes apparent that there will be a difference in arrival times for the differing frequency components of the pulse, which needs to be corrected for through a process known as dedispersing. The integral in the above expression is referred as the Dispersion Measure (DM), and is the integrated electron column density along the line of sight through which the pulse propagated. Through models of the ISM, which gives the average density of the free electrons, in the galaxy, the DM can be translated into a distance to the pulsar and allows for the galactic distributions of pulsars to be mapped. In the dedispersing process, the frequency band that is observed by the instrument is subdivided into a number of discrete frequency channels which can then be shifted by an amount of time to correct for the dispersive smearing, and the point where the pulse is completely dedispersed (i.e. no time delays remaining) gives the DM of the pulsar. An important consideration is the width of the frequency channels, in which there will still be some delay, corresponding to the second term in equation (3). In order to prevent this term from dominating, the number and width of the individual channels must be carefully considered, with the limit for the time resolution being the inverse of a single frequency channel width. Additionally, the step size of the dedispersing routine is an important consideration, for a step size that is too large will result in smearing and sensitivities for DMs that are in between each step and a step size too small will be computationally costly; a DM step that dedisperses with the total time delay equivalent to the data range is a reasonable first choice. There are of course a number of variants to the somewhat basic dedispersion routine described here, which can oftentimes improve the removal of the dispersive effects, such as the process of coherent dedispersion that completely eliminates dispersion through an analysis of the complex voltages received by the telescope and the ability to recover the original complex voltages of the radiation from the pulsar [17, 19, 46, 44, 50].

Although the dispersive effects can largely be eliminated through dedispersion, the time delay produced through scattering of the pulsar radiation is considerably more difficult to remove. Within the ISM, there are fluctuations in the density of the electrons and diffraction of the radiation can occur if there are fluctuations on scales less than $\lambda D^{1/2}$, where λ is the wavelength and D is the scattering region's size. Also, as the pulse traverses through turbulent portions of the ISM, the photons travel along different path lengths, thereby becoming scattered and undergo angular and temporal broadening. Since the scattering is essentially random, the distribution of their brightness will be Gaussian, and the original pulse is convolved with an exponential profile [16, 42]. This convolution produces the well-known scattering tail illustrated in Figure (2) and is described by the pulse broadening function:

$$PBF \propto e^{\frac{-t}{\Delta t_d}} \quad (5)$$

In this expression, Δt_d is the same scattering time lag given in equation (3) and is a function of the frequency of the observation and the spectral index of the pulse [5]. Its value can be estimated by:

$$\Delta t_d \propto SM^{\frac{6}{5}} \times v^{-\frac{22}{5}} \times D \quad (6)$$

This scattering time delay is clearly proportional to frequency and the distance D to the pulsar, in addition to the scattering measure:

$$\text{SM} = \int_0^D C_n^2 ds \qquad (7)$$

In this equation, C_n^2 is the spectral coefficient or a measure of the amount of turbulence within the ISM. As the frequency of the observations is decreased, the negative power in equation (6) will cause this time delay to grow and the pulse will be distorted to a greater extent, as shown in Figure (2). Furthermore, with increasing distance and consequently increasing dispersion measures, the effect will also grow, so distant pulsars will similarly be scattered to a greater extent. Should they become scattered to a very high degree, the matching of the pulse to a known "typical" pulsar shape in the match filtering step will not succeed and the pulse will not be detected in a standard search algorithm [17, 19, 31, 43].

Although the PBF is oftentimes unknown, the intrinsic pulse can be salvaged through deconvolution processes if some properties of the intrinsic pulse are assumed [5]. However, the scattering can be more easily reduced by simply observing at higher frequencies, which is why, despite the fact that pulsars were initially discovered at 81 MHz, most surveys performed today observe at much higher frequencies ranging from 350 MHz up to 1.4 GHz [33]. Accordingly, with the steep spectra of pulsars, which behave as $v^{-\alpha}$, where α is the spectral index, that generally makes them brighter at frequencies in the range of a few hundred MHz or less, there is tradeoff between higher fluxes at lower frequencies or less scattering at the higher frequencies which must be considered. Alternately, the match filtering process can be changed to include scattered pulse profiles, although this still requires deconvolution to study the intrinsic pulse and is generally a computationally intensive process [4, 43, 50].
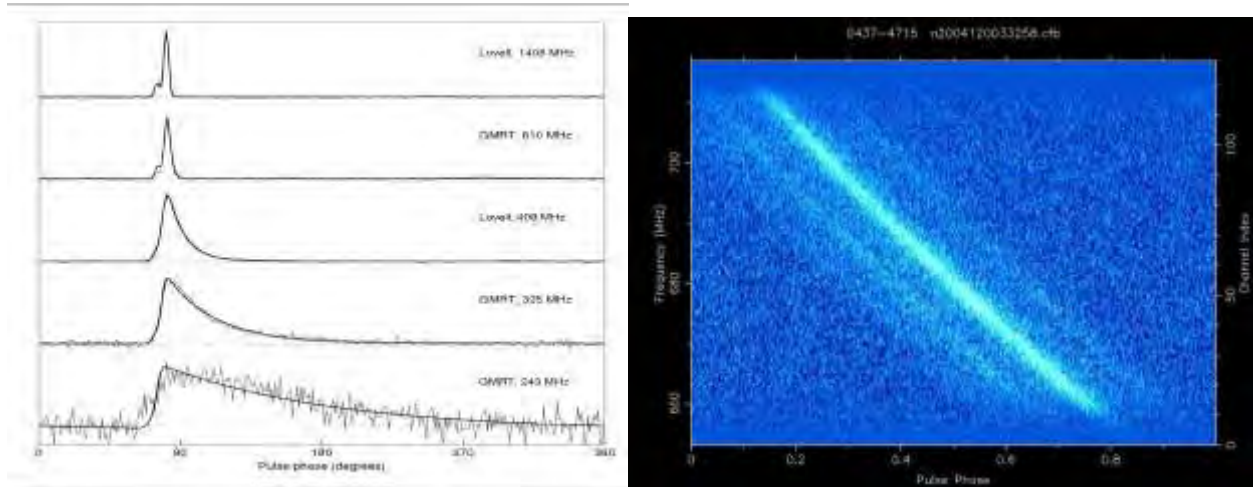

Figure (2): RIGHT: The effects of dispersion on a pulse, which plots frequency vs pulsar phase. There is a greater time delay for the longer frequency components of the pulse, which must be corrected for during analysis. LEFT: The effect of interstellar scattering on the shape of a pulsar's pulse, with higher frequencies at the top and lower frequencies at the bottom. The approximately Gaussian shape of the pulse is convolved with a decaying exponential form, thus distorting the pulse giving a scattering tail. This effect increases with decreasing frequencies [16, 18, 42, 64].

The remaining effect that causes considerable difficulty in the detection of pulsars, particularly in single pulse searches, arises from terrestrial radio frequency interference (RFI). Ever since the first radio telescope was turned towards the sky, RFI was observed, having been emitted by both natural sources, such as the atmosphere and human sources, including radio stations, cellular phones, faulty electronic

equipment, car spark plugs, and a vast assortment of other technologies that may produce both narrowband and broadband signals in the radio frequency band. These human RFI sources are oftentimes considerably stronger than most astrophysical signals and are usually most powerful at a DM of 0 pc cm^{-3}, thus having a greater effect on lower DM pulsars. As with the dispersion and scattering, RFI can be at least partially removed from the data, with such software as PRESTO and SIGPROC. These can "clip" or remove signals with large signal to noise ratios that are evidently not astrophysical, identify narrowband transient and periodic RFI that can sometimes appear to actually be a pulsar or RRAT detection, in addition to eliminating persistent signals. They then create a "mask" over the original data that removes any of these unwanted signals [10, 49, 50].

The natural sources of RFI arise in the form of either molecules in the atmosphere that absorb certain higher frequencies in the radio band and free electrons, which selectively scatter or absorb incoming photons. In the troposphere, both water and oxygen molecules have lower energy rotational transitions allowing for them to absorb photons at several different GHz frequencies, which has consequences for such instruments as the Jansky Very Large Array, and is the reason why most radio observatories are located at high elevations with little atmospheric water content. At the other, longer wavelength side of the radio atmospheric window, photons with frequencies less than the plasma frequency of the ionosphere's free electrons will not be able to propagate very well to the ground, and are primarily reflected back into space. As the presence of free electrons is highly dependent on the activity of the ionosphere, the ionizing radiation from the Sun makes the effect considerably more noticeable during the daytime, largely inhibiting observations below approximately 11 MHz. Both these sources of natural RFI cannot be removed and thus require considerations of the observing environment and finding opportune times to schedule observations in order to secure optimal conditions [68].

The Discovery of RRATs

The first detection of a RRAT was in a 2006 reanalysis of data from the Parkes Multibeam Pulsar survey (PMBS) that was carried out with the 64 m Parkes Observatory in New South Wales, Australia from January 1998 to February 2002 [45]. This survey observed the region around the galactic plane (|b| < 5 degrees and 50 degrees < l <2 60 degrees) at a center frequency of 1347 MHz (20 cm) and a bandwidth of 288 MHz. This survey's sensitivity was around 7 times higher than the surveys conducted previously at 400 MHz with other instruments, with a minimum detectable flux of 0.2 mJy for pulsars with periods of 0.1-2 s and dispersion measures less than 300 pc cm^{-3} [49, 51].

Whereas the initial analysis of the data from the PMBP survey searched for periodic signals and followed up on any candidates that were detected, the reanalysis carried out a single pulse search on the data and revealed 11 objects that pulsed on timescales of 4 minutes to 3 hours, with pulse widths ranging from 2 ms to 30 ms. All of these RRATs were not detectable in a periodic search and several of them were found to have particularly high flux densities between 0.1 Jy and 3.6 Jy, thereby making their flux densities second only to a few other pulsars known, including the Crab Pulsar's giant pulses. Follow up observations that had a total time on source ranging from 8 hours to 30 hours illustrated a considerable variation exists in the number of detectable pulses from these RRATs, with some having only 4 detected pulses and others having as many as 229. All of the RRATs were located at galactic latitudes |b|< 2, placing them very near the plane of the galaxy. Furthermore, the dispersion measures for these RRATs varied from a minimum of 88 pc cm^{-3} to a maximum value of 369 pc cm^{-3}, corresponding to distances from Earth of about 2.4 kpc to 5.5 kpc, thereby indicating that they are within our galaxy [51].

Despite their lack of being found in searches looking for periodic signals, a periodicity was found for several of these initial RRATs by determining the lowest common denominator for the time between the detection of each of their pulses, revealing that these neutron stars completed their rotations in a time range spanning from 0.4 s for the shortest to 7 s for the longest ones. Such values for the periods are in general longer than the majority of those determined from most other regular pulsars. In addition, period derivatives were also found, with their values being close to those of regular pulsars. Their location in the galaxy and these short periodicities, while long when compared to those of most regular pulsar periods, indicated that these sources were indeed emitting neutron stars, albeit a slightly different variety than those previously detected [23, 51].

From these initial detections, the currently accepted, although somewhat arbitrary, definition of a RRAT was developed, with an RRAT being defined as any neutron star whose beamed emission can only be detected in a search that looks for single bright pulses and not in a Fourier domain search that looks for periodic signals [11, 33, 51]. The arbitrariness lies in the fact that the detectability in a single pulse or periodic search varies from instrument to instrument and upon the lengths of observations. A less sensitive observatory may be unable to detect a period of nulling or lower emission activity in an X-ray isolated neutron star and thus detect it as a RRAT, even though its emission has not actually ceased, whereas it has been found that some RRATs are detected in periodicity searches in some observatories but not in others. Additionally, as RRATs are observed to generally have longer periods than most regular pulsars, the ability to detect them in a periodic search is less, so their being defined as an RRAT based on their non-detectability might simply be a selection effect resulting from this and not due to some intrinsic lack of emission. Therefore, some have suggested that RRATs be defined instead as those pulsars that are simply more easily found in single pulse searches when compared to their detectability in a periodic search. From this, one can define an intermittency ratio:

$$r = \frac{S/N_{singlepulse}}{S/N_{periodic}} \qquad (8)$$

An intermittency ratio larger than one would be more characteristic of what is expected from a RRAT, should one adopt this slightly more flexible definition. Again, however, this value depends on the observation in question, varying with observation length and many other factors, thereby leaving the definition of a RRAT still somewhat arbitrary. Further clarification on the exact nature of RRATs is likely required before a more systematic definition can be developed [11, 33].

Other Observations of RRATs

The 100 RRATs discovered thus far have largely been detected through the analysis of data from large scale blind pulsar surveys carried out by many of the major radio observatories. In 2010, Burke-Spolaor and Bailes reported the detection of 14 new RRATs in the more recent blind surveys with the Parkes observatory. This survey observed galactic longitudes from 5 degrees to 30 degrees, with the same longitude range and central frequency as the previous PMBS, but with an improved sampling time of 125 microseconds and pointings times that were only 4.4 minutes in length. These newly found RRATs are distributed throughout the galaxy in a manner that is similar to what is expected for pulsars and had pulse widths that were akin to those observed in the pulsars with periods close to those of these RRATs. This survey, however, did determine that despite these similarities, the RRATs were quite varied in their properties, with some potentially pointing to a connection between nulling pulsars and RRATs. PSR

J0735–62, for instance, had a fluctuating pulse strength, ranging from detected signal-to-noise ratios of 6 to 7.   The effect might not be intrinsic to the RRAT, but may be potentially produced by scintillation resulting from the pulsar's low DM. Follow-up observations lasting a total of 93 minutes were unable to detect any further emission in a single pulse search, but did observe a weak signal in a Fourier search. Several of the other 14 RRATs also were detectable in periodic searches, with intermittency ratios ranging from about 0.6 to 1.1, and are likely highly nulling pulsars whose longer periods and lengthy times of no emission prevented their detection in previous searches. One RRAT, PSR J1647–36, was observed to have a phase change of 5-10% for each time it restarted its emission, indicating that it might be a highly modulated pulsar, and others in this sample were found to be double or triple peaked [8].

In the original single pulse search carried out by McLaughlin et al. in 2006, it was reasoned that at least 50% of the RRATs that were present in the region surveyed by the PMBS were not detected as a result of radio frequency interference – it has the effect of potentially obscuring those RRATs with low dispersion measures due to it being strongest at a DM of 0 pc cm^{-3}. With the introduction of the superior RFI mitigation techniques by Eatough et al. in 2009 and with the development of more advanced computing facilities, the PMBS data were yet again reanalyzed by Keane et al. in 2010 and another 17 new RRATs were detected [32]. In its 2007 Drift Scan survey and the later Northern Celestial Cap Pulsar Survey (GBNCCP survey), the Greenbanks Radio Telescope added more than 18 new RRATs to the continually growing population. Both surveys took place at a lower frequency than many of the surveys with other telescopes, with observations at 350 MHz with a much higher sensitivity than many of those previous surveys, particularly to millisecond pulsars [7, 59]. Other surveys include the High Time Resolution Universe Survey (HTRU), a digital, all-southern-sky survey in conjunction with a Northern-sky effort by the Effelsberg telescope. It looked for pulsars and radio transients at a central frequency of 1352 MHz with slightly higher sensitivities for single pulsed emissions than the PMBS, identifying another 26 RRATs [9]. Arecibo's pulsar survey of the sky for galactic latitudes |b| < 5 deg and galactic longitudes 32 deg < l < 77 deg and 168 deg < l < 77 deg. increased the number of RRATs with more than 10 new detections at 1.4 GHz with 0.3 GHz bandwidth [20].

RRATs have also been studied more recently at the low frequency of 111 MHz during 2010-2012 with the LSA radio telescope at the Pushchino Radio Astronomy observatory. This study selected several of the RRATs that were found with the Parkes and Arecibo Telescopes at 1.4 GHz and looked for both single pulse and periodic emissions at this new frequency. They identified no single pulse emissions from any of the candidates, but did detect them in the FFT searches, with the maximum flux density from any of the targets not exceeding 100 mJy [44, 59]. With the relation between the flux and frequency of pulsars, the flux is expected to decrease with increase with the frequency, and with these low flux densities, this could serve as an explanation for the absence of periodic detections in many of the higher frequency searches.

In addition, a recent reanalysis of the GBT Drift-scan and the North Celestial Cap pulsar surveys located another 21 new RRATs, which were followed up by observations with both the GBT and the Low Frequency Array (LOFAR) to find timing solutions and superior position and DM measurements. The LOFAR observations were carried out at a center frequency of 150 MHz with 80 MHz of bandwidth, whereas the GBT follow-ups again probed 350 MHz along with 820 MHz, each with a bandwidth of 100 MHz and 200 MHz respectively. The RRATS found in this analysis are essentially similar to those of other surveys and discoveries with the GBT, with similar spatial distributions to regular pulsars, but periods that are generally longer (240 ms to 3.4 s). The pulse rates with the GBT's lower frequency observing band ranged from a lowest rate of 20 per hour up to a maximum of 400 bursts per hour, whereas the burst rate for the LOFAR

observations was substantially less, demonstrating the instrumental dependence of this measurement [30].

While the vast majority of RRAT detections and follow-up observations are obviously carried out in the radio portion of the spectrum, as that is where the coherent pulsar emission primarily exists, as with regular pulsars, other qualities of RRATs can be observed at shorter wavelengths. To date, no RRATs have been observed to have an optical counterpart, as is the case for a few regular pulsars, although no large scale optical observations of detected RRATs have been performed to date. However, RRAT J1819–1458, a young highly magnetized neutron star with spin properties similar to those of magnetars, was detected at X-ray wavelengths during a 30 ks remnant with the Chandra X-ray Observatory observation of a coincidently nearby supernova. From the small number of detected photons (524 +/- 24) the spectrum was well-fitted to a blackbody model, indicating its origin as thermal emissions. Within a 3-sigma upper limit, there was no evidence found for any variability on timescales ranging from 3.2 seconds to 5 days in the X-ray flux of J1819–1458. Evidence was also found for an X-ray pulsar wind nebula surrounding the RRAT [34].

A follow-up 94 ks observation was carried out with the XMM Newton telescope in 2013, simultaneously with radio observation follow-ups with the GBT, Effelsberg, and the Parkes telescope at frequencies of 1-2 GHz. It was determined that J1819-1458 possesses a blackbody spectrum with kT on the order of 130 keV, indicating an age of approximately 10^4 to 10^5 years. The spectrum was found to possess broad absorption spectral features, first observed in the earlier Chandra observation, which can be attributed to a variety of effects, including the ISM and other effects more directly related to the RRAT. With the longer pulsar period (4.6 seconds), X-ray timing measurements could be carried out and a correspondence between the pulses in the X-ray observations and those of the radio observations is believed to exist, with the X-ray pulses being thought to be emitted in phase with the radio pulses [34, 52].

What are RRATs?

With their only being discovered recently and with the difficulty in carrying out observations due to their oftentimes long periods of no emission, the mechanism behind the transient pulsing of RRATs remains as yet undetermined. Observational evidence points to a number of potential origins and similarities to many of the other subclasses of pulsars, but no definitive evidence has been found to either satisfactorily prove or rebuke most of the theories that have been advanced thus far. One observational trait that hints at their origin is in the timing measurements that have been carried out on many of the RRATs. Accurate determinations of both their periods and spin down properties permit comparisons to be made between RRATs and other pulsars, such as nulling pulsars. If these appear to indicate that RRATs possess some common trait that constrains their properties, such as their ages, magnetic fields, and their basic emission mechanism, then some theories may be able to be excluded. If a relation between RRATs and some other type of pulsar be found and if many of their properties also prove to be of a specific type, then it would be possible to partially alleviate the issue of the supernova rate being insufficient to account for RRATs alongside regular pulsars, as RRATs would simply represent an evolutionary stage in a pulsar's life cycle.

McLaughlin et al. found timing solutions for 7 of the 11 RRATs found in the first PMBS, and of these, 3 possessed both magnetic fields and spin-down rates which were comparable to those found in magentars and X-ray isolated neutron stars, and they determined that 2 others with periods that clearly places them near the pulsar death line. Indeed many RRATs have been found to exhibit periods longer than those of the general population of pulsars [49]. This fact points to the possibility that RRATs might be some form

of transition state of pulsar that are very near the point where their rotation periods are too long to sustain emission. In other words, as a pulsar grows older, its rotational velocity decreases, and the requirements to continue the emission of the beams become more difficult to fulfill. When near this point, it has been postulated that this dying pulsar might not simply shut off its emission all at once, but could begin a period of transient or single pulse emissions like what are observed in RRATs [23, 69].

This idea is somewhat further supported by the detection of a white dwarf pulsar in 2005 that pulsed on a timescale of 77.13 minutes, maintaining its pair production temporarily through an inferred surface magnetic field of about 10^9 G. This "pulsar" reactivated for a period of time before again going silent, likely corresponding to a short term period of pair production, and it seems reasonable to presume that similar conditions might occur on neutron stars [71]. For such neutron stars, pair production may be temporarily reactivated should smaller sunspot-like magnetic field regions merge near the polar region, providing sufficient energy for emission. The most obvious issue with this interpretation is that not all of the RRATs observed have periods and period derivatives that are near the death line on the P-Pdot diagram and are, therefore, not likely to be pulsars of a considerable age. One possible explanation is that the current dipole models for neutron stars are not adequately describing the magnetic field, such that the actual magnetic field is less than what is predicted and RRATs could still be nearly dead or reactivated pulsars [70].
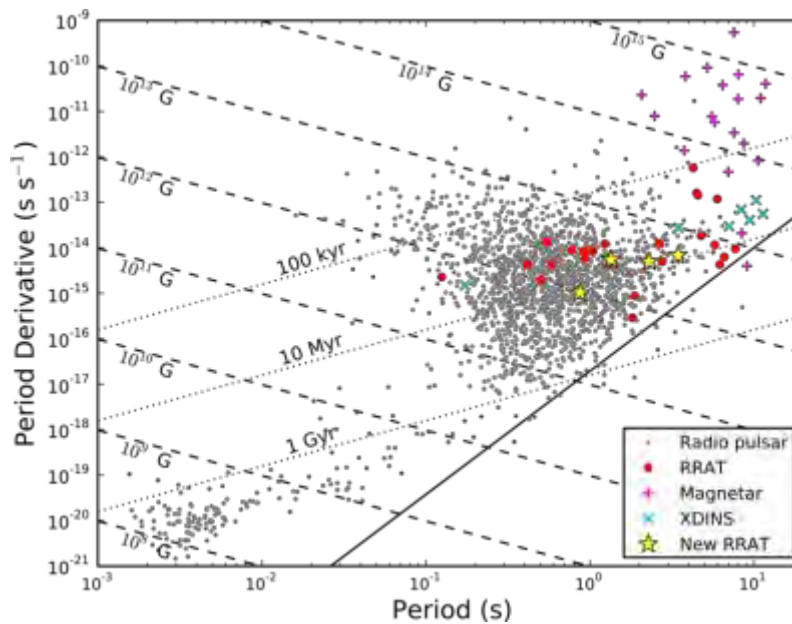

Figure (3): The location of many RRATs on the P-Pdot diagram. The solid line represents the pulsar death line where emission is expected to die out, although the exact position and width of this line is not entirely well defined [29].

An alternate theory describing this discrepancy was suggested by J. Arons in 2000 to describe nulling pulsars, interpreting the spin properties of RRATs as an off-center magnetic field in a dipole arrangement, such that there is a difference in strength in each pole's field. If RRATs are a case where the weaker side is observed, then they would appear to possess weaker magnetic fields than regular pulsars, which would be those neutron stars that are oriented such that the stronger pole is facing us. For most of the time no emission would be observed due to the weak magnetic field on this side. RRATs would, consequently, not

be older than any of the other older pulsars that populate the "death valley," but simply appear so, meaning that their thermal emissions would be equivalent to that of a pulsar of lesser age. This fact could serve as a potential differentiator between the various existing theories [70].

Zhang et al also suggested an entirely different method for the observed behavior of RRATs based on the idea put forth by Dyks et al in 2005 to describe the behavior of the mode switching nulling pulsar PSR B1822-09. Instead of near death or reactivated pulsars, this model interprets RRATs as simply being a geometric effect produced by a reversal of the direction of emission of the radio beam. For regular pulsars, what is observed is only the outward pointing beam as it crosses our line of sight, but if the beam should reverse, the inward pointing beam would then be visible corresponding to the observed nulling period of the RRAT. The difficulty in this model is determining what causes the direction reversal. A potential origin may exist in oscillations of the electric field in the gap regions, with the result being that there is a periodic acceleration effect for the electron positron pairs in the magnetosphere. The pair creation from energetic photons would move both inwards towards the surface, thus transferring energy and heating the polar cap regions, and outwards to generate the escaping pulsar beam [28, 70, 71].

P. Weltevrede et al identified a number of similarities between the properties of RRATs with those of the pulsar PSR B0656+14, a nearby (0.288 kpc) "middle-aged" pulsar with high energy emissions being detectable in single pulse searches. The period, spin down properties, and magnetic field strength that is expected of this pulsar are also very near to those observed in RRATs thus far. The bursts from PSR B0656+14, which have fluxes 420 times larger than the regular pulses it emits, are not believed to be produced through the same emission mechanism as the bright pulses from other pulsars, due to their longer timescales, no X-ray component, and non-power law energy distribution, clearly ruling out a strong surface magnetic field. P. Weltevrede et al therefore suggested the idea that this pulsar may in fact be a typical RRAT that is near enough that we can detect the regular emissions through periodic searches – they predict that should PSR B0656+14 be at least 12 times further away, only 1 burst per hour would be detectable. Other RRATs are, in this interpretation, simply bursting middle-aged pulsars that are further from us such that the normal emissions are too faint to be observed [24, 67, 69].

Unusual behavior in the emission processes of pulsars do not represent the only probable explanation for the sporadic nature of RRAT pulses. In a decidedly different view from the dying pulsar and direction reversal mechanisms, J. M. Cordes & R. M. Shannon instead interpreted RRATs, as well as nulling pulsars, which are, in this scenario, less extreme version of RRATs, as being neutron stars with a circumpulsar debris field orbiting above it. The idea of such a field to exist around a neutron star has been in place for some time before this explanation of transient pulsar phenomena was suggested. Fallback of material from the supernova explosion is possible and should it have low mass and exist close to the neutron star, then planetary body formation is prohibited (by tidal forces in the latter case) and only smaller rock-sized objects on the order of 1 m would form. As this debris enters the light cylinder of a neutron star, the conditions within the region are thought to be able to heat, and thus evaporate, or ionize the debris, which will then produce a change in the distribution and movement of the magnetosphere's plasma. This could either quench the pair production that is crucial to pulsar radio emissions or in some cases actually provide the necessary energy to reactivate it. The input of material from the orbiting field is required to occur periodically with the interactions between the debris, such as collisions between fragments, gravitational herding of some fragments by others, or by the anisotropic emission of photons from the neutron star's surface. Those objects pushed into the light cylinder will be most affected by the greater forces present in the gap regions, where the charged particles will be accelerated by the electric fields.

These can either act in the same manner as the pairs produced in standard pulsar emission models or they can reduce the magnitude of the electric field in the gap regions, thus potentially inhibiting or completely shutting down any existing emissions [20].

While there is no concrete evidence that appears to favor any theory over any of the others, several observational examples exist that support some hypotheses, and ideas on how to distinguish which one might be the most plausible also exist. In the reactivation model, due to the fact that the neutron star is of considerable age, there should be very little in the way of X-ray thermal emissions during the times that the emission is turned off. Additionally, in the off-center dipole explanation, the weaker side's inwards beam would also not be expected to have a pole that is significantly heated, so only a small X-ray flux are would be expected in this scenario. For the hypothesis that RRATs are a beam direction reversal effect, on the other hand, the RRATs are comprised of mostly middle aged pulsars that are still actively emitting, so X-ray thermal and nonthermal emissions from the magnetosphere are to be expected. Indeed, X-ray emissions from regular nulling pulsars have been detected in numerous observations by XMM Newton and Chandra, with hotspot regions having been reported. X-ray observations would consequently determine whether or not there exist large X-ray fluxes from RRATs thus distinguishing if either of these two models is the correct interpretation. Indeed, as mentioned above, the X-ray detection of PSR J1819–1458 was best modeled by a thermal blackbody spectrum and not by nonthermal spectrum and did not indicate the likelihood of hotspots. This is primarily consistent with the Zhang et al's off-center dipole model and is not described by the direction reversal model [34, 70].

For the circumpolar asteroid model, both direct observations of the field itself and inferences on its existence based upon the observable effects it may cause on the neutron star's spin properties could provide evidence as to its validity. So far, observations of pulsars with known planetary companions at infrared frequencies have not detected any emissions, but disks around young, hot neutron stars are expected to be visible. Radio reflections of the pulsar's radio beam emission from asteroids of sufficient size are also expected, with the strongest reflections potentially reaching about 10 μJy. Again, unlike the reactivation model that would not be expected to emit at high energies, the heating, ionization, evaporating, and subsequent reactivation of the pulsar will likely emit in the X-rays. Finally, the asteroids will introduce spin fluctuations, as objects entering the light cylinder will "spin-up" and the neutron star must correspondingly slow down. The charges entering the magnetosphere must also exert a torque on the neutron star, which may be detectable [20].

Determining what the true nature of the differing observed pulsing characteristics of RRATs represents an important problem that requires consideration, due to the consequences that exist depending upon their origin. As mentioned above, the original PMBS survey was thought to have only identified roughly 20 % of the RRATs that existed in the region of the sky that was observed. Assuming similar estimates for other surveys, the number of RRATs in regions surveyed can be as many as 5 times the number of actual detections, thereby increasing the total number of pulsars that emit at radio frequencies in the galaxy (currently estimated at about 10^5 pulsars) by several times. If RRATs are actually a distinct form of pulsar that forms independently of regular pulsars, and would therefore not be described by the above models, they would be counted in addition to the number of regular pulsars. Given the need for the birth rates of the various populations of neutron stars needing to add up to the supernova rate in the galaxy, the presence of RRATs would require a substantial increase in that supernova rate. Indeed, the maximum supernova rate was estimated by Keane et al to be 3 century^{-1}, whereas the neutron star birthrate required to account for RRATs as a distinct class was estimated to be 5.8 century^{-1} [31].

This appears to point to one of several possible conclusions. The first potential explanation for the discrepancy would be that the estimates on the regular pulsar birth rate being in error, although this number represents the most well studied of all the individual birth rates, having the least uncertainty in the measurements. The population of RRATs might be overestimated to a very large degree; given that they were only discovered recently and their properties are still not as well understood as those of regular pulsars, this may be the more likely explanation for solving the insufficient supernova rate. Indeed, it has been shown that if the lifetimes of RRATs were to be increased by only a single order of magnitude to approximately 50 Myrs, the required number of supernovae to produce the $2x10^5$ estimated RRATs would still be too large compared to what is estimated, but would be within a more acceptable range of 3 century^{-1} [31].

While the birthrates of the other subclasses of neutron stars, such as magnetars and XDINS could also be in error, the interpretation of RRATs as being an evolutionary stage in a regular pulsar's lifecycle has the potential to reconcile the neutron star birth rates and supernovae rates. In this scenario, for which the above theories on RRAT origins would be valid, only a single neutron star subclass's birth rate would be required to account for the presence of several neutron stars types and the total birth rate would as a result be substantially less than the combined birth rates of the individual populations [31].
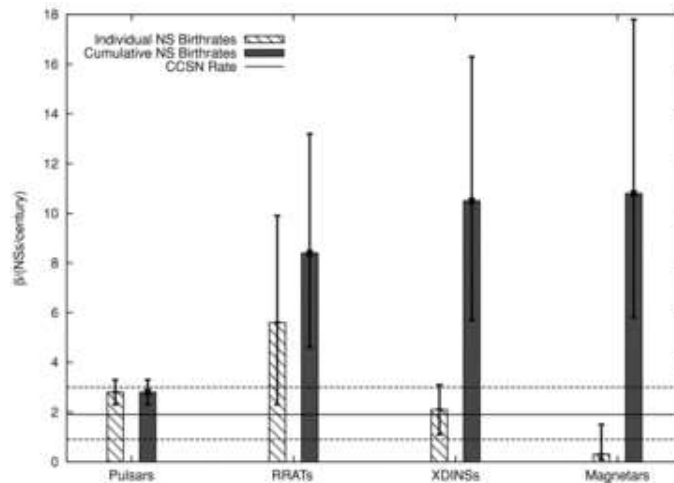

Figure (4): Estimates on the birth rates of Neutron stars in our galaxy along with the estimates of the supernova rate [31].

The Long Wavelength Array

The Long Wavelength Array (LWA) is a University Radio Observatory that is currently operated by the University of New Mexico, with assistance from a number of other participating institutions, including Los Alamos National Laboratory, Naval Research Laboratory, Jet Propulsion Laboratory, Virginia Tech, as well as support from the California Institute of Technology, the National Radio Astronomy Observatory (NRAO), and the Air Force Research Labs. The observatory currently consists of a single station (LWA1), or a single array of dipoles, that came online in late 2012. It is co-located with the Jansky Very Large Array (JVLA), due to the area's suitability for radio astronomy and in order to make use of the JVLA's computing facilities. Another station is now in construction about 70 km from LWA1 and at least 51 more are planned to be built in the future, which will allow for higher spatial resolution and interferometric observations to be carried out [29, 61].

The original idea for the Long Wavelength Array dates back to 1984, with R. Perley and W. Erickson advancing the idea that a high resolution synthesis array with wide bandwidth capabilities that would carry out useful studies of the universe at wavelengths longer than a meter could be constructed for at a low cost in the vicinity of the VLA and utilize its already present computing capacities. Unlike at higher frequencies (higher than about 300 MHz), observatories operating at these lower frequencies do not make use of the single-dish design utilized by the VLA, Arecibo, the GBT, due to the fact that wavelengths are far larger than the dish size, thus limiting the angular resolution and sensitivity obtainable. For such observatories, it is more efficient and cost effective to create an array of dipoles, for which the effective collecting area of the array is proportional to the square of the wavelength, allowing for these arrays to gain higher sensitivities than single dishes. Several arrays can then be constructed with larger baselines of several kilometers or more, permitting them to be used as interferometers, much like the way that the Very Large Baseline Array is comprised of individual single dishes [51].

Observatories that could carry out science at these wavelengths were in very few numbers prior to this proposal, due to the prohibitive effects of the ionosphere and due to the computing requirements to correlate the input from the large number of antennae that are required. Some earlier observatories include the 26.3 MHz array starting operations in 1959 which probed low frequencies with a sensitivity of about 10 Jy and a collecting area of 26000 m^2, the 74 MHz Interplanetary Scintillation Array that primarily made studies of solar cycles with a 50 Jy sensitivity, and the electronically steerable Tee-Pee-Tee array that could operate at frequencies between 20 MHz and 125 MHz, which observed galaxy clusters, solar astrophysics, and the galactic plane at 1 Jy sensitivities. With the exception of a few of these preexisting arrays, such as the aforementioned IPS array, all had their longest baselines less than a few kilometers; longer baselines were prevented by the ionosphere's scintillating and refracting effects on longer wavelengths that varies from location to location, thus making calibration across the entire array difficult. Furthermore, none of the preexisting arrays were capable of forming a beam that was smaller than 1 degree, thereby significantly limiting the science that could be done with these instruments, as most galactic and extragalactic sources require much smaller beams in order to be resolved [53, 61].

There are also a number of arrays in operation today that operate at similar low frequency ranges to that of the LWA. The Low Frequency Array (LOFAR) is a large scale radio observatory built and operated by Netherlands Institute for Radio Astronomy (ASTRON) that was planned as early as 1990 and first came online in 2007, and now has several stations across several nations in Europe. It utilizes 25,000 omnidirectional dipoles and can observe at frequencies between 10 to 240 MHz. It is currently the most sensitive instrument in the world at these lower frequencies and has an approximate effect collecting area of 30,000 m^2. Its primary science drivers, many of which are shared by the LWA, involve studies of transient radio signals, investigations of the sun and Earth's atmosphere, as well as cosmological studies, such as the search for the epoch of reionoization through studies of the 21 cm hydrogen spectral line at high redshifts. In addition, there is the Murchison Widefield Array (MWA) in Australia that operates between 80 MHz and 300 MHz and is comprised of 128 "tiles" with 16 dipoles each. The JVLA is also currently implementing a long frequency observing mode through the placement of dipoles near the foci of several of its dishes, allowing for observations of 50-80 MHz to be carried out. The Square Kilometer Array (SKA) has a planned low frequency component that is sensitive between 50 MHz and 350 MHz that will consist of 250,000 wideband dipoles with spiral arm baselines out to a distance of 50 km, which would allow for high spatial resolution [61, 69].

Consequently, it was R. Perley and W. Erickson's suggestion that a radio observatory composed of simple Yagi design or helical design dipoles with a frequency range between 30 MHz and 180 MHz and a bandwidth of about 5 MHz should be constructed and would prove scientifically beneficial. The primary targets of interest for this array would include studies of objects that radiate via plasma processes, including the Sun, Jupiter, and pulsars, in addition to extragalactic sources such as radio galaxies, quasars, galactic halos, all of which have steeper spectra making them particularly suitable for studies at meter wavelengths. Supernovae remnants, HII regions, and flaring stars were also potential targets of interest for a high resolution, low frequency array [54]. The Long Wavelength array inherited many of these original ideas and science drivers, while also adding to and improving on them in a variety of ways, such as in the design of the antennae and in the introduction of all-sky imaging modes [29, 61].

The current LWA1 station consists of an array of 256 stands, or one set of two orthogonal antennae within a 100 m by 110 m ellipse. The stands have the antennae angled downwards by 45 degrees in order to improve their sensitivity at lower altitudes; for a hertz dipole the angle at which the maximum sensitivity is obtained is 90 degrees to the axis parallel to the length of the dipole, so by tilting the dipole by 45 degrees, a larger portion of the sky can be observed at greater sensitivities. With these antennae, the LWA1 station can observe at any frequency between 10 MHz and 88 MHz with a maximum bandwidth of 19.6 MHz (about 16 MHz are usable due to the decreasing bandpass sensitivity at the edges of the band) and two linear polarizations. The station can produce up to four independent and steerable beams at one time, with each able to observe at two frequencies or tunings, with a beam width smaller than 3.2 degrees at 74 MHz, or it can phase up every antenna stand and observe for long periods of time in a narrowband all-sky monitoring mode or for short time periods with a wideband all-sky mode. In the beamforming mode, data can be recorded in two separate modes, known as regular and spectrometer modes, with the latter having 32 individual channels and an averaging time of 20 ms, thus providing a much reduced data rate when compared to the regular observing mode. Finally, there are two separate bandpass filters, referred to as the split filter, which limits the frequencies to those between 30 MHz and 88 MHz, and the full filter setting that allows for all the frequencies over the entire LWA band to be admitted. The split filter exists to reduce the effects of RFI on the observations, which can dominate the lower end of the band [29, 61].

Figure (5): The first station of the Long Wavelength Array (LWA1) and a close-up individual stand consisting of 2 orthogonal dipole elements angled down by 45 degrees to improve sensitivity at mid elevation angles [61].

Data from LWA observations are recorded on to disk drives that are at the site, but data can be conveniently transferred to the LWA User Computing Facility (LWAUCF), a computing cluster consisting of 6 nodes located at the nearby VLA control building. Users can connect remotely to and make use of the

LWAUCF, which is preloaded with a large variety of software designed for diverse science applications, including the LWA's own software library, to reduce their data and carry out analysis. Reduction and analysis can also be carried out on a number of computers at the University of New Mexico that have the same software installed as the LWAUCF if the need should arise.

With pulsars being one the primary fields of study behind the LWA's construction, the observatory has carried out a sizable study of pulsar properties at these low frequencies; thus far, the LWA has detected more than 50 pulsars through their periodic emissions that were previously identified in higher frequency surveys, with 3 of them being millisecond pulsars. Observations of these pulsars are generally carried out in the split filter settings on two beams with the tunings centered at frequencies of 35.1 MHz and 49.8 MHz for one beam, and 64.5 MHz and 79.2 MHz for the other beam. With a bandwidth of 19.6 MHz for each tuning, the results can be combined during analysis and the properties of the pulsar can be determined over the entire frequency range used. Due to the heightened effects of interstellar dispersion on pulses in the LWA frequency band when compared to its significantly smaller effects at the higher frequency pulsar searches, in addition to the array's high time and frequency resolution, the LWA is capable of determining many of the ISMs properties to a much higher level of accuracy through pulsar observations. This involves placing much tighter constraints on the dispersion measures of pulsars and therefore their distances from us as inferred from this value, in addition to how this dispersion measure varies with time.

In addition to these targeted observations of already known pulsars, there is an ongoing effort with the LWA to carry out an all-sky survey to detect pulsars, RRATs, and other transient radio objects that may might not have been found in other surveys, potentially due to their intrinsic properties making them easier to find in the 30-88 MHz region. This survey is highly computationally intensive due to the very small DM step size required for the data searches, as a DM step size comparable to those of other surveys is insufficient to counteract the greater scattering and dispersive effects of the ISM, and has yet to detect any new sources.

Although no sky model for the LWA has been developed thus far that would allow for absolute flux calibration, the system equivalent flux density for the polarization parameter stokes I is known, and varies as a function of frequency and elevation angle, attaining a value of about 3kJy at zenith. This system equivalent flux density or SEFD is a measurement of the instrument, sky, and background to the system noise. The SEFD is approximately constant for frequencies between 30 MHz and 88 MHz, but fluctuates strongly outside of this region. Additionally, it increases significantly with lower elevation angles, due to the change in the array's effective area [58]. Unfortunately, the uncertainty in the SEFD's measurement is on the order of 25 % for the zenith angle, and for the remainder of this discussion, an uncertainty of 50 % is assumed due to the lower elevations for which the RRATs were detected. The SEFD allows for the flux densities of individual pulses from RRATs or other transient sources to be determined utilizing the expression:

$$S = \frac{(SNR)(SEFD)}{\sqrt{N_{pol}\Delta f W}} \quad (9)$$

Here, Δf is the total bandwidth of the observations, W is the FWHM of the pulse, and N_{pol} represents the number of polarizations for the observation, which, for the LWA pulsar observations would have a value of one, which is Stokes I. The width of the pulse is not the intrinsic width, but the broadened width after

dispersion and scattering. The minimum flux that is detectable for a given pulse width and SNR at an elevation in the vicinity of 50 to 60 degrees is plotted for each of the two bandwidths utilized in figure (6) below [25].
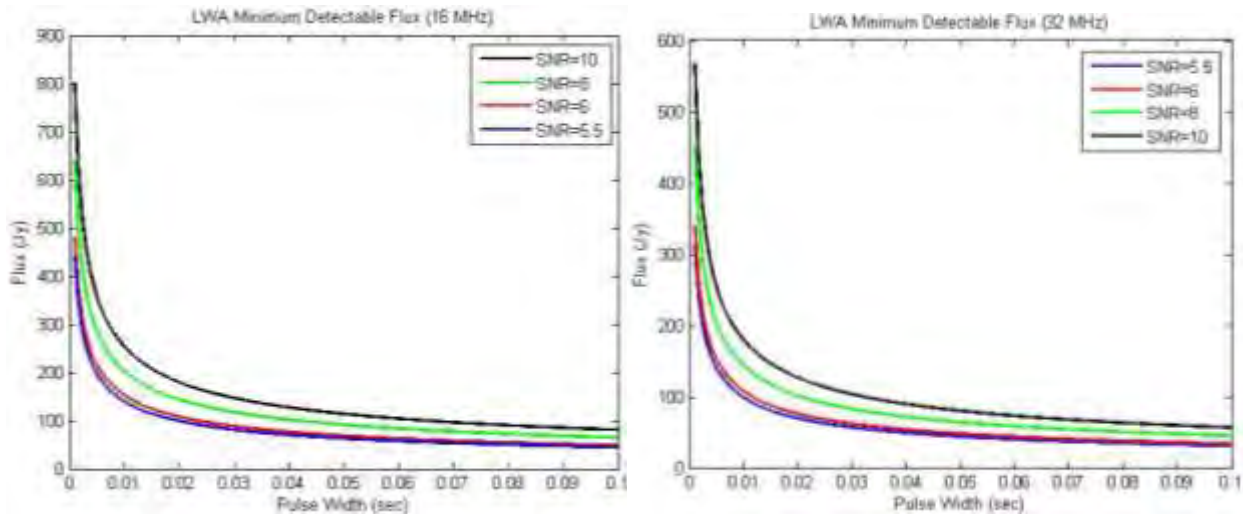

Figure (6): LEFT: minimum detectable flux of a single pulse with the LWA for different detected pulse widths and SNRS for a bandwidth of 16 MHz. RIGHT: same plot, but for a bandwidth of 32 MHz. Error bars are not shown for clarity, but are on the order of 50 %.

Additionally, the part of the expression above without the SNR is the rms noise of the instrument for a given pulse. For the LWA, the rms noise as a function of detected pulse widths and excluding other instrument or RFI factors is illustrated in figure (7) below for the two different bandwidths utilized. As with the minimum detectable fluxes shown above, the rms noise decrease with the greater pulse widths and bandwidths.
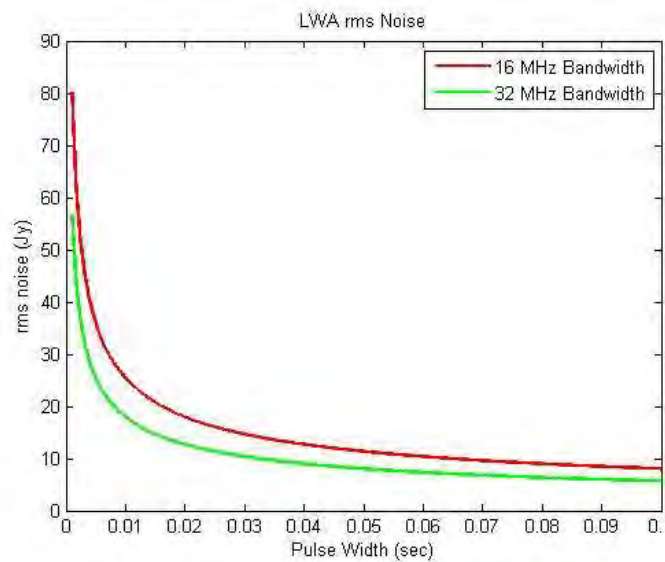

Figure (7): The estimated rms noise of the LWA for bandwidths of 16 MHz and 32 MHz. As with figure (6) error bars are not shown for clarity, but are on the order of 50 %.

The Potential for RRAT Observations with the LWA

The LWA's success at re-detecting pulsars that were originally found by higher frequency observations serves to provide some motivation for carrying out a study of previously identified RRATs with the instrument. This idea is further reinforced by the fact that in the surveys carried out at lower frequencies, more new RRATs were identified than those that looked at higher frequencies. While this may be the result of some systematic effect, such as a higher sensitivity (the GBT observations were done with a higher sensitivity than many of the surveys carried out at even higher frequencies with other telescopes), it might also be indicative of a steep spectrum for these transients. Regular pulsars themselves have steep spectra, so RRATs might also follow this trend. Should the as yet unknown RRAT spectral index prove to be very steep all the way down to the LWA's observable frequency band, then they would be easier to detect, thus making the LWA a suitable instrument for their study. Finally, when compared to the number of hours that can be devoted to long-term and timing measurements of RRATs, the LWA is capable of dedicating considerably more time than any of the previous, highly subscribed instruments, thereby allowing for the potential to track any changes that may occur with individual targets. Indeed, a large number of RRATs do not yet have values for their periods, as doing so requires many observations over the course of several months; with the LWA, should a RRAT have a sufficient number of detectable pulses, performing these lengthy timing observations, as well as measuring the dispersion measures and the changes in the dispersion measures to a very high degree of accuracy, does not constitute a problem. Adding to this advantage is the fact that, since many the RA/Dec positions of many RRATs are not well constrained due to limited time on targets, the LWA's large beam size makes precise coordinates largely unnecessary, thus making the RRATs more likely to be found within the beam and detected.

There do exist a number of issues that may inhibit the LWA's ability to perform useful scientific observations of RRATs. As mentioned above, the RRAT spectral index down to the low frequencies has not yet been determined, so the possibility exists that there may be no significant advantage at observing down to the lower frequencies over higher frequencies. Additionally, the LWA's sensitivity limit is sizably larger for its frequency band (about 5 Jy) than the sensitivity of the other telescopes that have observed RRATs at higher frequencies (on the order of only a few mJy). Compounding upon these potential roadblocks, the sky at the lower frequencies probed by the LWA is accompanied by its own share of traits that have the effect of limiting RRAT studies. At the lower end of the frequency band around 20 MHz the ionosphere is very active, particularly during the day, thereby making daytime lower frequency observations difficult to salvage. Furthermore, with its inverse relation to frequency, the dispersive nature of the interstellar medium will distort the shape of the incoming pulses far more than is experienced with the higher frequency surveys, with the result being that distant pulses will be smeared so much that they might not be detectable during the match filtering process during the data analysis.

The first intention of these RRAT observations with the LWA is to simply determine whether or not these objects are detectable at low frequencies, and if they are, how do their properties compare with those determined in their detections at higher frequencies. Whether or not they behave as RRATs or as regular pulsars at low frequencies and whether they have similar pulsing rates are questions that this study intends to answer. For those that are detected, finding out if their pulses are of similar width and shape to that which is already known is another point that will be clarified. For those that are not detected, what intrinsic properties of RRATs might have led to these non-detections and what does this tell us about RRATs or pulsars in general are additional considerations.

RRAT Observations with the LWA

The RRAT observations carried out by the LWA are divided into two separate observing runs separated by approximately one year, each characterized by different frequencies, observing times, and radio frequency interference removal tools. The first of these observing sessions took place from mid-2013 to early 2014 and selected 10 RRATs as targets, which were selected based upon the criteria that they had sufficiently low dispersion measures (less than 50 pc cm^{-3}), that no previous timing observations had been performed with any other telescope, and that multiple pulses had been confirmed in the initial discovery, as shown in Table (1). Two of the array's beams were used providing an effective central frequency of 64 MHz and a bandwidth of 32 MHz. The first observations were two hours in length and those with detections were followed by 30 minutes observations. The observations and data reduction of this run were carried out by Dr. Maura McLaughlin and Rossina Miller at West Virginia University.

Table (1): RRATs that were observed with the LWA in the first observing run, along with their dispersion measures, periods as measured by other instruments (unless otherwise noted), RA, DEC and LST range.

Source	Dispersion Measure (pc cm^{-3})	Period (s)	RA	Dec
J0203+70	21	1.35/0.746 (LWA)	02:03	70:23
J0337+79	15	2.056	03:37	79:02
J0447-04	30	4.38	04:47	-04:42
J0957-06	27	1.72	09:57	-06:17
J1439+76	21	0.947	14:39	76:55
J1537+23	15	3.45	15:37	23:50
J1610-0128	27	1.3	16:10	-01:28
J1704-04	43	0.238	17:04	-04:40
J1944-10	31	0.409	19:44	-10:17
J2324-05	15	0.869/0.870 (LWA)	23:24	-05:07

The second observation run, which constitutes the subject of this study, began in August 2014 and ended in March 2015 with the intention of observing a total of 18 RRATs: those that were selected in the 2013-2014 run were chosen to be re-observed, as many were not detected, and another 8 were added. These RRATs are listed in Table (2) along with some of their properties. The constraints on the selection of these newer additions was not as stringent as the first set, simply due to the fact that there were insufficient RRATs that fit the earlier run's restrictions. The upper limit on the dispersion measure was raised to 100 pc cm^{-3} and RRATs with previous timing solutions were also chosen. Every RRAT in both sets also satisfied the criteria that their declinations must be above -20 degrees to ensure that the LWA's lower sensitivity and higher SEFD at decreasing elevations did not significantly impact target detectability. For this second observing run, the setup of the observations was the same as that utilized in the successful pulsar observations with the LWA, with two beams, or four tunings, at central frequencies of 35.1 MHz, 49.8 MHz, 64.5 MHz, and 79.2 MHz, each with bandwidths of 19.6 MHz (although again only 16 MHz are considered usable due to the bandpass shapes). All observations of the second run were scheduled at night to limit both the ionosphere's effects and the level of RFI. All took place in the LST time range where the RRATs were at the highest elevation possible. The gain setting for each observation was chosen to be 7, again the same value as that of the regular pulsar observations. Finally, each observation was one hour in length and the RRATs were observed twice on separate nights with no particular spacing between the

sessions chosen, resulting in a total time on target of 2 hours. This is much longer than the pointing times for many of the surveys that found the RRATs picked here, thereby increasing the likelihood of a detection.

Table (2): RRATs that were added to be observed with the LWA in the second observing run, along with their dispersion measures, periods as measured by other instruments (unless otherwise noted), RA, DEC and LST ranges.

Source	Dispersion Measure (pc cm^{-3})	Period (s)	RA	Dec
J0053+69	90	1.16	00:53	69:38
J0054+66	15	1.390	00:54	66:50
J0105+53	57	0.0886	01:05	53:50
J0628+09	88	0.548	06:28	09:09
J1610-17	52	--	16:10	-17:50
J1623-08	60	0.503	16:23	-08:41
J1753-12	73	0.405	17:52	-13.00
J1848-12	88	0.414	18:48	-12:47
J1850+15	24	1.383	18:50	15:32
J2225+35	51	0.94	22:25	35:00

Data Reduction and Analysis

Following the observation, the data were primarily transferred to the LWAUCF (some was analyzed on computers at UNM, but the processes are exactly the same), where reduction and analysis was performed. The analysis tools utilized is the PulsaR Exploration and Search TOolkit (PRESTO) software that was developed by Scott Ransom, with assistance from a number of others. PRESTO is largely written in ANSI C, with many additional python components being added later, and has been successful in detecting more than 300 pulsars to date. Its primary role was to detect millisecond pulsars, but has been utilized for all kinds of pulsar observations, including the regular pulsar observations made with the LWA and in the analysis of pulsar X-ray data. Consequently, PRESTO contains all of the important steps for standard pulsar studies, including RFI removal tools, dedispersion tools, single pulse and periodic search routines, period folding software, and more. Plots of the DM vs time, DM vs SNR, and a number of others are created allowing for visual confirmation of detections and files containing information such as times and corresponding SNR's are also generated.

Many of the analysis steps for these RRATs in PRESTO are the same as those utilized to study regular pulsar data, with the primary difference being in the replacing of the usual periodic search routines with single pulse search techniques. First, the raw data were transferred to the LWAUCF and through the use of PRESTO's writePSRfitsMulti2.py module, the data were converted into the standard PSRfits file type. This particular version creates a .fits file of equal duration for each of the beam's tunings, which are then combined into one fits file for all the tunings using the code combine_LWA2.py. Following this, the RFI finding script rfifind.py, with an integration time of 10 seconds, was utilized to create the mask that would be applied in the later analysis steps. If the observation was found to be plagued by considerable RFI, only the upper two tunings were combined and used, as the RFI was considerably less at the higher frequencies, due to the atmospheric contribution to RFI's inverse dependence on frequency.

Once the RFI mask is generated, the fits file can then be dedispersed using the code prepsuband.py. The data were divided into 128 subbands and dedispersed with a step size of 0.001 pc cm^{-3}, which makes full use of the LWA1's high time resolution to get the value of the DM down to such high accuracies and helps to reduce the errors introduced in the dedispersion process. While a larger number of subbands would further reduce these errors, this number of subbands was chosen as a balance between error reduction and computation time. The vast majority of RRATs have an uncertainty in dispersion measures on the order of +/- 1 pc cm^{-3}, with some having reported errors on DM as large as +/- 8.7 pc cm^{-3}. With the small DM step size required and given the fact that a DM range larger than those reported was searched to maximize the chance of a detection, the computational time to cover these ranges therefore increases by a fair amount necessitating the smaller subband number. The code prepsubband.py outputs several output files, including .dat files and .inf files which contain the dedispersed data and information about the observation in question. Additional noise reducing processes were then performed on the data to lessen the likelihood of false detections. Finally, these output files were then searched for single pulses with PRESTO's singlepulse.py, producing a number of .singlepulse files containing a list of the times, DMs, and signal-to-noise ratios of any candidates. These candidates were then plotted to determine how they appear with the varying of the many free parameters, including DM, SNR, and the number of detected pulses.

The resulting plots were then examined and any potential candidates were noted. A candidate consists of any bright signal detected at a small range of DMs and at a particular time. The SNR of the pulse must be greater than the SNR of the noise, which generally attains a value of 5. The "pulse" should fall off with DM sharply, thereby allowing for many detections to be somewhat easily ruled out as RFI. Any pulses that appeared to be candidates were compared with the RFI signatures at zero DM for similar times and with other RFI signals at similar DMs at the same time. If there was substantial RFI occurring at this time, but no other, the detected pulse can readily be overlooked. If little RFI that is coincident with any detections is observed or if the observation had considerable RFI, but at a many different times throughout the observation, then the potential detection was examined further. This involves examining the pulse shape through a python program written by Dr. Kevin Stovall, which simply plots the pulse's SNR vs pulse phase. If the pulse shape matched what is expected from a pulsar and is not clearly RFI, then follow-up observations were carried out for confirmation. A similar code utilized a python fitting routine to fit the pulse to a Gaussian profile and the best fit parameters were found, allowing for the full width at half maximum to be approximated and thereby translated into a pulse time width.

In addition to the basic steps that were carried out and listed above, most of the RRATs were also examined in periodic searches, particularly those that were actually found in single pulse searches. This procedure was motivated not only by the fact that in follow-up observations with higher frequency instruments, some RRATs were later identified as regular pulsars, but also due to the fact that one our detected RRATs was also found in a periodic search with the LWA. The periodic search method utilized the same conversion to fits format routines, as well as the same RFI masking and dedispersion methods, with the sole exception being the replacement of the singlepulse.py code with PRESTO's accelsearch.py, accelsift.py, and prepfold python programs. Furthermore, for the RRATs of high DM, where any pulses will be distorted from the expected Gaussian distribution to a large degree, a python program written by Dr. Kevin Stovall for use on the Crab Giant pulses that performed match filtering on the .dat files from PRESTO against "typical" scattered pulses was utilized, to overcome the fact that the singlepulse.py will not consider these types of pulses in its searches of the data.

Results

Of the 18 RRATs observed with the LWA, only 3 confirmed detections have been made, with 2 from the 2013-2014 observing run and an additional detection being added by the 2014-2015 observing run. The RRATs that were detected are J2324-05, J0203+70, and J0054+66, all of which were originally discovered with the Greenbanks Telescope in its 350 MHz sky surveys [24]. The general properties of the LWA detections of these 3 RRATs are each summarized in table (3) and described in more detail in each of the following sections below.

Table (3): Summary of the properties of the 3 RRATs detected with the LWA.

Source	LWA Peak SNR	LWA Detected DM (pc cm^{-3})	LWA Pulsing Rate (hr^{-1})
J0054+66	8.29 (2nd run)	14.556 +/- 0.003	0.66
J0203+70	8.3 (1st run)	19.998	0.5
J2324-05	19 (2nd run)	14.960 +/- 0.003	40

J2324-05

PSR J2324-05 was the first RRAT to be detected with the LWA and has been confirmed in both observing runs with the different observation configuration. Due to the beam combinations of the second observation, the detection was significantly improved over that in the first detection, resulting in a larger pulse rate and SNR, as is shown in figure (8). This RRAT was originally found in the 2007 Green Bank Telescope's 350 MHz Drift scan survey described previously, with a DM of 15 +/- 1 pc cm^{-3} at a discovery SNR of 40 and a burst rate of 120 hr^{-1} [24]. In comparison, the LWA's detection DM was 14.960 +/- 0.003 pc cm^{-3}, with a peak SNR of 19, thereby making it the highest SNR RRAT the LWA has detected. The pulsing rate was also much higher than the other two detections, with the 32 MHz observations yielding a rate of 50 hr^{-1}, compared to the first observing run's 12 hr^{-1}.
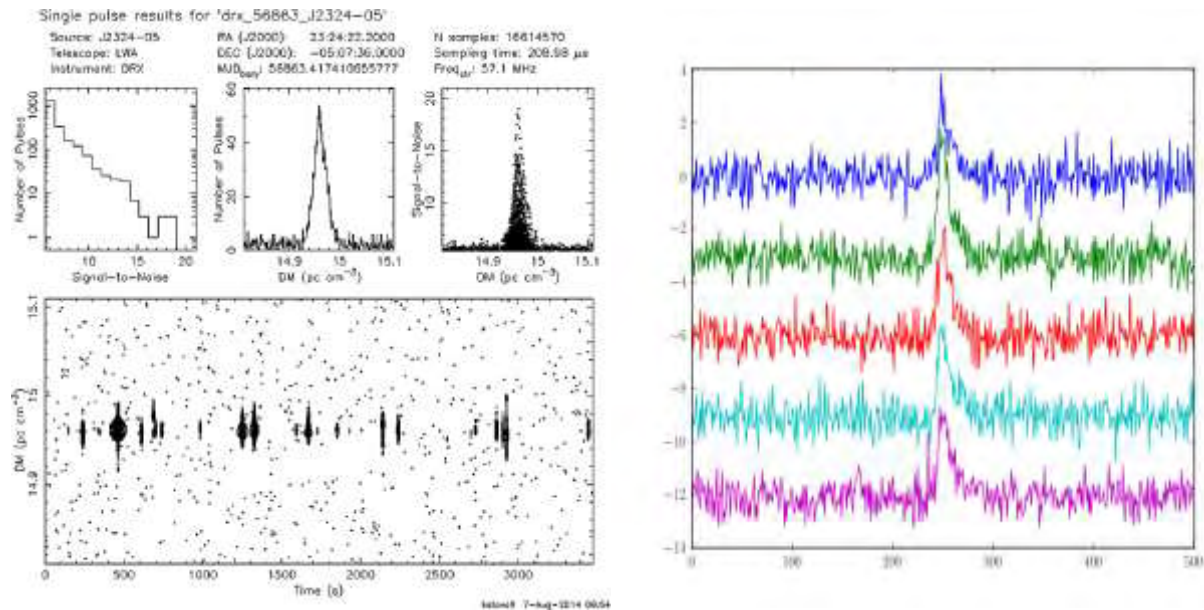

Figure (8): The detection of the RRAT J2324-05. The image on the left shows the results given by PRESTO's singlepulse.py code. The image on the right are the pulse profiles for a number of pulses.

Pulse width for the pulses in the individual frequencies were found and are listed along with their SNRs, fluxes, and the spectral indices derived from the upper two tunings (chosen due to the lower scattering in the higher frequency tunings) in table (4) below. J2324-05 was not detected in the periodic searches carried out on each of the detection observations, regardless of its high pulse rate and SNR. A period was found, however, using the method described previously of determining the least common multiple value between detected pulses, with the result being 0.870 s. One pulse on the 35.1 MHz frequency tuning showed an apparent strong secondary peak component as illustrated in figure (9), with other peaks potentially having a similar, though smaller second peak as well. This is not believed to be produced by RFI, due to the lack of major RFI in the observation, and as a result of the secondary peak's presence in several pulses in each observation, which occurred at different times and would therefore not likely be affected by the same narrowband RFI.
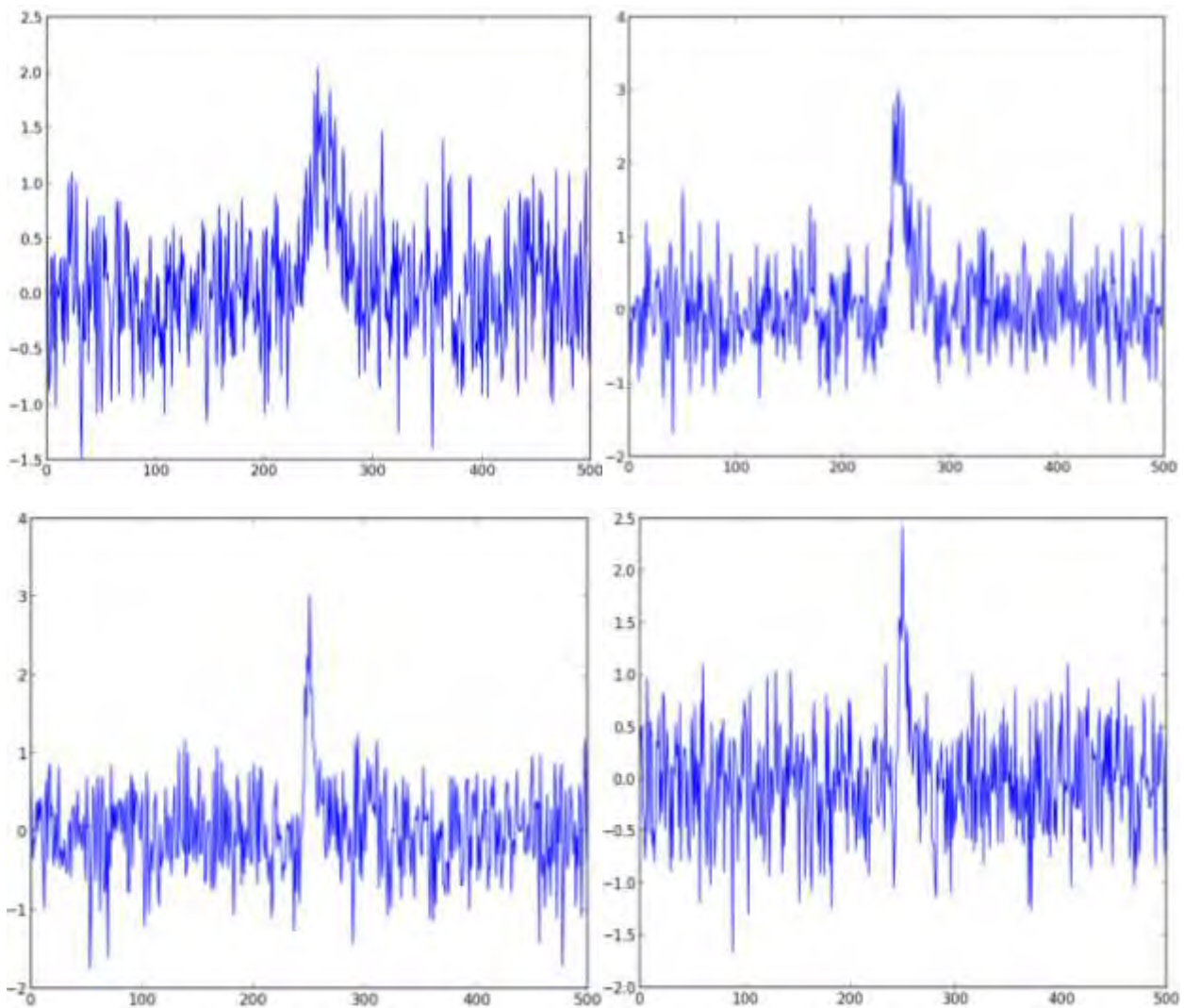

Figure (9): Pulse profile demonstrating a possible secondary peak, whose size varies with frequency and from pulse to pulse. Top Left: 35.1 MHz. Top Right: 49.8 MHz. Bottom Left: 64.5. Bottom Right: 79.2

Table (4): Various Parameters for several detected pulses at different frequencies for J2324-05. The greater pulse widths and pulse width errors, in addition to the lower SNR at lower frequencies arises from the frequency dependent scattering. The spectral index is calculated from the top two tunings.

Pulse 1 Properties			
Frequency (MHz)	FWHM (ms)	Peak SNR	Flux (Jy)
35.1	90.082 +/- 35.809	8.83	74.27 +/- 39.74
49.8	51.338 +/-6.329	14.11	157.86 +/- 100.46
64.5	31.161 +/-3.355	13.19	189.41 +/- 94.04
79.2	27.285 +/-6.702	9.82	150.70 +/-76.69
Spectral Index:	1.11 +/- 3.46		

Pulse 2 Properties			
Frequency (MHz)	FWHM (ms)	Peak SNR	Flux (Jy)
35.1	83.752 +/-52.584	6.25	54.75 +/- 32.03
49.8	68.001 +/- 14.171	11.61	112.86 +/- 56.98
64.5	44.010 +/-0 9.040	11.25	135.94 +/- 68.56
79.2	28.917 +/- 9.922	7.90	117.77 +/- 61.56
Spectral Index:	0.70 +/- 3.54		

Pulse 3 Properties			
Frequency (MHz)	FWHM (ms)	Peak SNR	Flux (Jy)
35.1	100.835 +/- 67.409	7.35	58.68 +/- 34.99
49.8	50.151 +/- 10.023	10.95	123.95 +/- 62.45
64.5	26.307 +/- 5.493	9.37	146.45 +/- 73.91
79.2	27.025 +/- 9.232	8.34	128.61 +/- 67.20
Spectral Index	0.63 +/- 3.54		

J0203+70:

This RRAT was first detected in the Greenbanks North Celestial Cap Survey also at 350 MHz and was identified in the first 2013-2014 LWA observing session. The initial detection DM in the GBT survey was 21 +/- 1 pc cm^{-3}, whereas the LWA's DM was 19.998 pc cm^{-3}, with a signal-to-noise ratio of 8.3. The GBT's discovery SNR was 16 and its discovery burst rate was 150 hr^{-1} [24]. Only one pulses was detected in the first 2 hour observation, as shown in figure (10), which leads to an estimated detectable pulsing rate of 0.5 hr^{-1}.
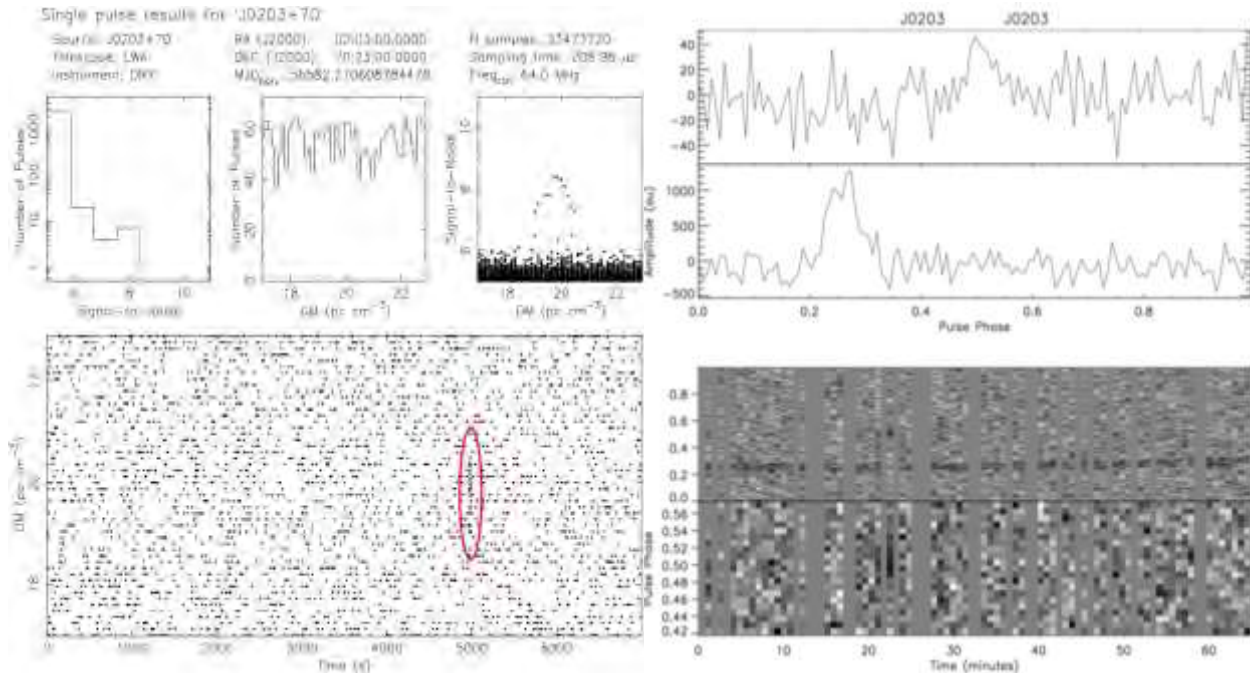
Figure (10): LWA detection plot of J0203+70 in the first observing run. The RRAT was also detected in a periodic search, as shown on the right. No further observations with the LWA have been able to detect either periodic or single pulse emissions.

Interestingly, J0203+70 was also detected in the periodic search, making it the only of the 3 RRATs the LWA has detected to be found by normal pulsar searching methods in this study. Its period from this detection was measured to be 746 ms, which is in disagreement with the more recently found value of 1.35 s at higher frequencies. Adding to the somewhat differing nature of this RRAT, when compared to the 2 others detected with the LWA, subsequent attempts to detect J0203+70 in at least three separate observations in either single or periodic searches during the second observing run have proven unsuccessful, with the reason as to its non-detection in both remaining unclear, although its single pulse search non-detectability likely originates from its low pulsing rate. The flux density and pulse widths of this RRAT are not reported here due to the non-detection in the second observing run.

J0054+66:

This RRAT was one of the 8 new RRATs selected for observing in the second observing session, and, as with the other two RRATs that were discovered with the LWA, was first detected with the GBT, in its Survey of the Northern Galactic Plane for Radio Pulsars and Transients again at 350 MHz. Its initial GBT detection DM was at 15 +/-1 pc cm^{-3}, with a burst rate of 240 hr^{-1} and a flux density of 15 mJy. Additionally, its period was measured with the GBT and was found to be 1.390 s [24]. The pulse profile had a width on the order of 20 ms and was observed to have a secondary component, which was also apparent in the LWA observations [39]. A total of 6 observations with the LWA have been carried out on this RRAT, with 3 yielding detections and the others no observable emissions. The number of detectable pulses in each of the observations varied depending upon the frequency and bandwidth for which the observation was examined, with two of the 57.1 combined bandwidth observation yielding only one detected pulse per

observation and one detecting 2 pulses as is illustrated in figure (11). The detections at the other individual frequencies without the combined beam also vary in the number of pulses detected, with some finding none, whereas the 64.5 MHz tuning of the same observation that detected 2 pulses at 57.1 MHz also detected 2 pulses within the hour long observation. The secondary component is not clearly visible in most of the detections, with only one observation providing having a clear secondary peak, as shown in figure (12).
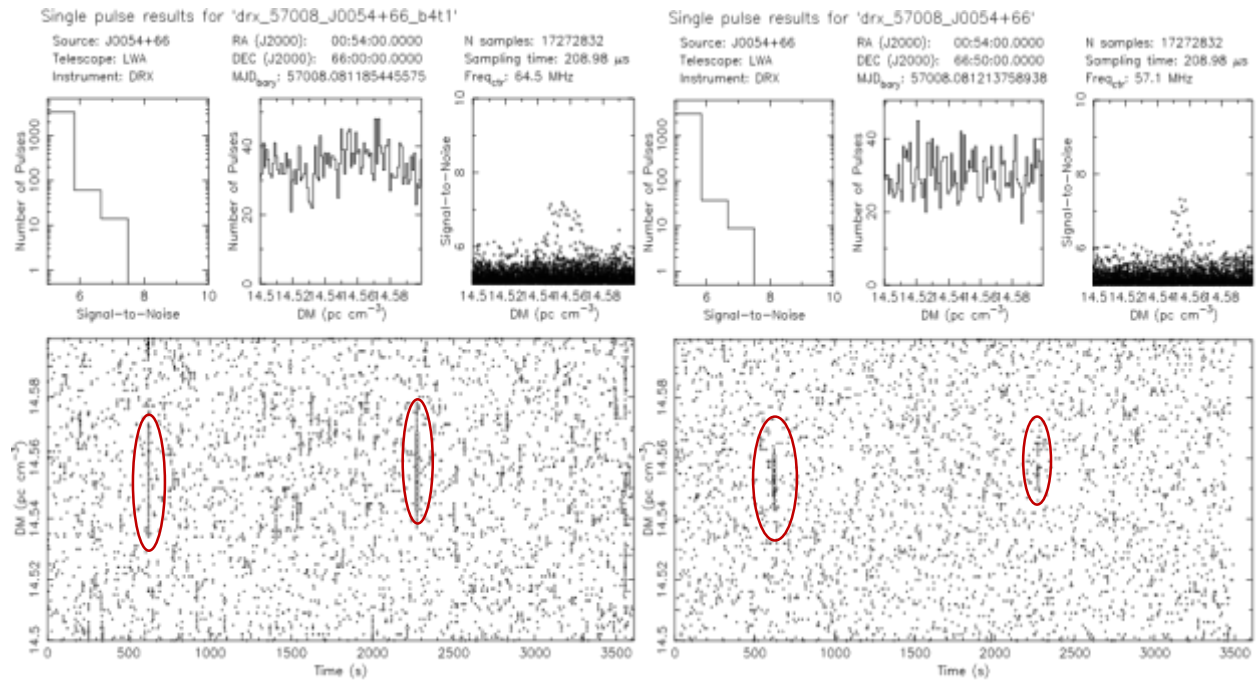

Figure (11): Comparison of the 64.5 MHz (16 MHz bandwidth) observation with the 57.1 MHz (32 MHz bandwidth), illustrating the detection of two pulses each observation, with the brighter pulse in the first image on the left appearing dimmer in the second image on the right.
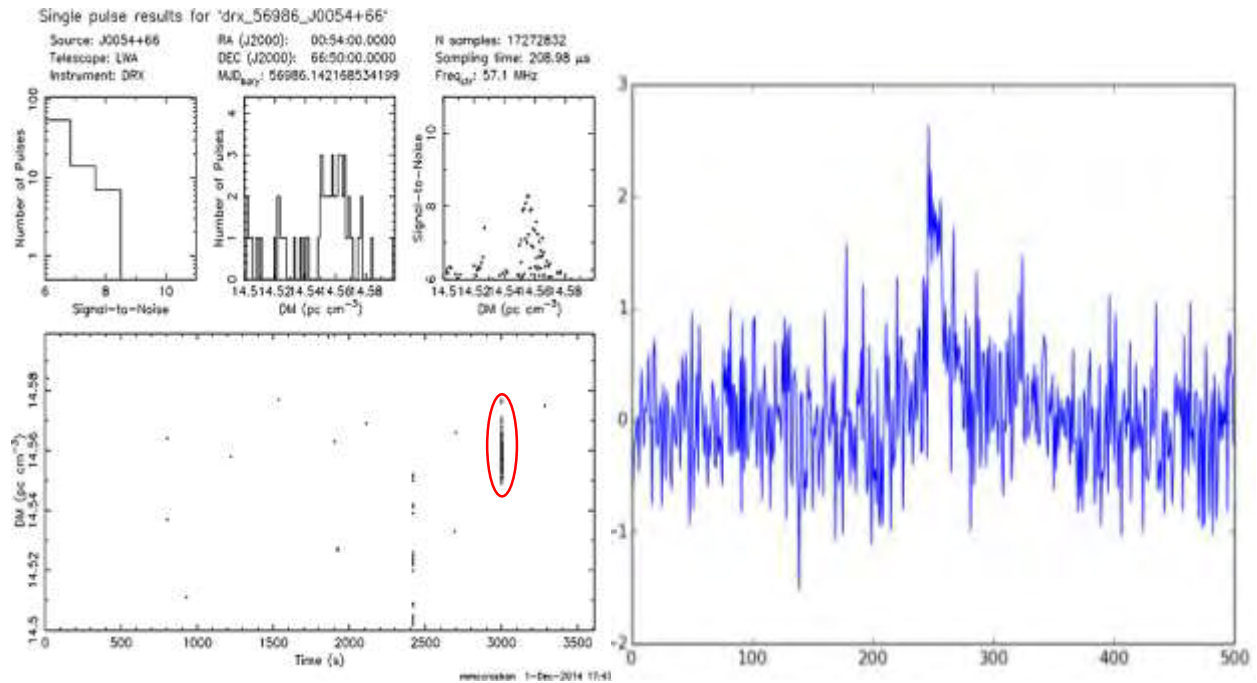
Figure (12): One of the many detections of the RRAT J0054+66 made with the LWA, with this one corresponding to the SNR=8.29 pulse in the 32 MHz bandwidth observation. Visible in the pulse profile on the right is the secondary component or peak, which is not visible in the pulse profiles from all of the observations.

The LWA's dispersion measure did not change significantly from observation to observation or pulse to pulse in those observations that had multiple detections, with the DM attaining a value of 14.556 +/- 0.003 pc cm^{-3}. These variations likely do not originate from any intrinsic changes in the pulsar or the interstellar medium, but are most probably only variations in the noise level due to their small magnitudes. The pulse widths and the measured SNRs, however, do change to a greater extent, with the SNR for the 32 MHz bandwidth observations varying from a lower limit of 6.64 to an upper bound of 8.29 and the pulse widths being in the range of 45 ms to 61 ms. The 16 MHz observations show similar variations, with the properties of these listed in table (5). Unlike the DM fluctuations, those of the SNR have a greater chance of being the result of some intrinsic property of the RRAT, the ISM, or the ionosphere's properties, since the elevation angle of the RRAT was the same for all the observations, indicating that the LWA's sensitivity should have remained nearly constant for each detection.

The variations in SNR and pulse widths result in a derived flux density that is also variable, with values between about 55 Jy and 62 Jy for the 32 MHz observation and much larger values in the range of 70 Jy to 120 Jy for the individual tunings. From these flux values and those of the GBT's 350 MHz observation, a spectral index can be derived, with an average of the fluxes from the 32 MHz observations giving a value of 4.563 +/- 0.244. The spectral index for each of the 16 MHz bandwidth detections is given in their corresponding tables below.

As with J2324-05, J0054+66 was not detected in any periodic searches with the LWA – an additional 2 hour observation was performed with the intention of improving the detectability in a periodic search and

to get a better estimate on the pulsing rate, but no single pulse or periodic emissions were detected even in this longer session.

Table (5): Various Parameters for the pulses detected from J0054+66 for the three different observations and two different bandwidth settings. NOTE: Two pulses were detected from observation 3, but the width and flux are not given for the weaker pulse in the 16 MHz observation due to the very low SNR in the pulse, which gives large errors in the Gaussian fitting. Observation 2 did not have any detectable pulses in the 16 MHz bandwidth.

32 MHz Pulse Properties			
Observation	FWHM (ms)	SNR	Flux (Jy)
1	61.359 +/- 22.245	8.29	59.99 +/- 33.38
2	55.195 +/- 31.729	6.64	55.20 +/- 32.40
3	45.100 +/- 24.380	7.32	61.18 +/- 38.58
3 (pulse 2)	32.823 +/- 19.332	6.14	60.75 +/- 39.24

16 MHz Pulse Properties Observation 1			
Frequency (MHz)	FWHM (ms)	Peak SNR	Flux (Jy)
35.1	None	None	None
49.8	77.190 +/-46.656	8.10	73.91 +/- 42.79
64.5	None	None	None
79.2	None	None	None
Spectral Index:	4.36 +/- 0.30		

16 MHz Pulse Properties Observation 3			
Frequency (MHz)	FWHM (ms)	Peak SNR	Flux (Jy)
35.1	None	None	None
49.8	None	None	None
64.5	22.059 +/- 7.515	7.14	121.87 +/- 63.66
64.5 (pulse 2)	See note above	5.65	See note above
79.2	None	None	None
Spectral Index	5.32 +/- 0.31		

Discussion

The detections of only this small fraction of RRATs out of this sample is likely the effect of not only the intrinsic properties of the targets and the limits of the LWA1 station, which may make detections difficult at these lower frequencies through various ways, but is also due in part to poor observing conditions. The latter affected the 2013-2014 observing run considerable more than the 2014-2015 observing run, due to the observations being carried out in the daytime. As described in the description of pulsar searches above, the ionosphere becomes more opaque to higher frequencies during the day and human produced RFI is also somewhat more pronounced [69]. This resulted in all but a few of the observations being completely swamped by unwanted interference which could not be removed via RFI excision tools such

as rfifind. With the move to nighttime observing, only a few sessions were rendered unusable by RFI, with most being almost entirely devoid of interference other than some short duration burst-like signals across all DMs. Unusable observations in the second run were simply re-observed as the RFI was not persistent. One observation of J0957-06 in the first run tentatively detected a pulse at nearly the correct DM, but the majority of the observations was unusable due to RFI and the nature of the pulse could not be confirmed. The two observations of this RRAT in the second run were nearly RFI free, but did not detect any pulses at the DM of the pulse in the first run.

The much lower level of RFI in the 2014-2015 observing session means that the cause of the large number of non-detections must result from something other than obscuring radio interference, and is likely the result of both the observatory's characteristics and the intrinsic properties of the RRATs themselves. Several reasons behind the non-detections can be inferred from the qualities observed in those detected and extended to those that were not found. For instance, all three are low DM RRATs with somewhat low detected pulsing rates compared to their pulsing rates in the GBT detections, but with fairly differing observation elevation angles and periods, potentially ruling out a systematic effect resulting from the LWA's sensitivity being too low due to the target's zenith angle. The first interpretation that can be derived from these facts is that perhaps most RRATs possess a smaller pulsing rate at these lower frequencies, with the consequence being that the two hours of observations utilized here may have been insufficient in length to detect any emissions from most of the targets. A slightly different idea, based on some of the models for RRAT emission mechanisms, would be that the flux densities of the majority of the pulses emitted by these transient pulsars is too small to be observed with the currently limited LWA sensitivity. Those that are observed are only those few pulses that have notably higher than normal flux densities than most of the other pulses, a situation similar to the giant pulses model for RRATs put forth by P. Weltevrede et al. Alternatively, there may be no underlying more regular emission at all and either most RRATs do not emit at all above the LWA's minimum detectable flux density or most are too far away such that they are too faint that even their bright pulses cannot be seen [67].

This idea of RRATs being too far away or on average too dim to be observed with the LWA is somewhat supported by the low DMs of those that we actually detected. While pulsars of DMs up to 50 pc cm^{-3} have been detected with the LWA, these were with periodic searches where the sensitivity is boosted through the folding of the data – no such sensitivity advantage exists for the single pulse searches, so if the individual pulse's flux densities are too small, there is little chance of being able to observe them. With that said, none of the RRATs observed in periodic searches were detected either, including J1850+15 and J0628+09, both of which are now also classified as regular pulsars, as each has been identified in a periodic search at higher frequencies, with the initial single pulse only detections being thought to be a consequence of high levels of pulse-like RFI in the discovery observations. J0628+09 has a very high DM of 99 +/- 2 pc cm^{-3}, meaning that its non-detection in either LWA single pulse or periodic searches could originate from the pulsar being far too scattered at these low frequencies to be detected in either the regular or scattered searches. J1850+15, on the other hand, only has a DM of 25 +/- 8.7 pc cm^{-3}, which is only slightly higher than the DM of J0203+70 and much less than the highest DM regular pulsar found with the LWA, so the non-detection is currently unexplained other than by a perhaps too short observation time. A follow-up investigation of this particular pulsar might prove useful.

While the above arguments do appear to substantiate the idea of most RRATs being too dim to be detected with the current LWA's capacity, some of the non-detections were also low DM RRATs, indicating that in general most must also be too faint to be detected even at these shorter distances from Earth.

Should this prove to be the correct interpretation, this would allow for some constraints on RRAT flux densities and spectra in the LWA frequency band to be determined; the detected flux from these RRATs must be less than the rms noise of the LWA as shown in figure (7). However, with an error in the vicinity of 50 % on the SEFD for the LWA, not much can be derived from this, other than the fact that those RRATs that were detected are brighter at these lower frequencies than they are at higher frequencies, there is little that can be determined about their intrinsic properties without refining the SEFD measurements. With the steep spectra of pulsars in general, this greater flux is not a surprising result, although it does potentially allude to similar physical origins for both the RRAT emissions and regular pulsar emissions.

The alternate theory of RRATs having variable fluxes is also somewhat substantiated by the detections of J0054+66 and J0203+70, which display some variability in their pulsing on top of their RRAT transient pulsing. The changes, despite being small in magnitude, in the former's emitted flux might indicate that what we are seeing are only the brightest pulses, and most of the remaining pulses are not bright enough for the LWA to detect. Indeed, in the observation that detected two pulses, the SNR varied by a factor of 1.19 from the first pulse to the next in the 32 MHz observation and by a similar value of 1.26 in the 16 MHz observation, although the SNRs were reversed in the latter's case. The lack of any sort of detection in the follow-up observations of J0203+70 may illustrate that the RRATs emit at these lower, currently undetectable flux levels for considerable lengths of time.

Also worth consideration is the appearance of additional components or secondary peaks/notches in both of the RRATs that had their pulse profiles examined. J0054+66 was known to have such a secondary component in its 350 MHz, whereas no such structure has been reported in J2324-05 thus far, although its non-detection in observations at 350 MHz or higher would be unsurprising due to the near non-visibility of the other notch at the LWA's highest frequency tuning of 79.4 MHz. Should the existence of this additional structure in J2324-05's pulse profile prove not to be attributable to RFI, which, as described previously, does not appear to be the cause, since the second peak appears in many different pulses, then this may represent a trait shared by perhaps a large number RRATs at low frequencies in general. The second peak in normal pulsars is often attributed to emission from a different region or part of the radio beam, with the larger spacing between peaks at lower frequencies corresponding to these frequency components being emitted at higher elevations from the neutron star.

With essentially no other studies of RRATs at the frequencies utilized here, it is difficult to ascertain which of the above ideas represents the explanation behind the non-detections; it is certainly possible that both play a role, in addition to other causes that have not been considered. Therefore, the usefulness of future observations of RRATs with the LWA is somewhat challenging to evaluate, although concretely determining whether or not most RRATs actually emit in this low frequency band will help constrain their spectra further and consequently their emission mechanisms. With the greater chances of detecting lower DM pulsars in the 10-88 MHz band, continuing with a more focused study of RRATs with low DMs near those of the RRATs that were detected, with considerably more hours spent on individual targets would likely prove successful in establishing their visibility in the 30-88 MHz region. Furthermore, with the addition of new stations to the LWA in the near future, the increase in sensitivity would likely assist in a larger number of detections of RRATs, should most be simply too dim to observe currently. Indeed, the largest difficulty currently in this study is characterized by the high errors on the measurements of the fluxes, pulse widths, and consequently the spectral indices. By improving upon both the accuracy of the Gaussian fitting program and the SEFD would increase the scientific values of these measurements by a substantial degree and would be allow for a much better characterization of RRATs at low frequencies.

Finally, a coincident observation the RRATs detected with the LWA by both a higher frequency instrument and the LWA might provide evidence as to whether the pulsing mechanisms are the same for the two different bands.

Conclusion

We have observed 18 RRATs that were first identified in surveys with higher frequency instruments at substantially lower frequencies between 30 MHz and 88 MHz with the first station of the Long Wavelength Array. Of the targets observed and analyzed in both single pulse and periodic search routines, 3 RRATs were detected and the pulse widths and flux densities were estimated for each. Additionally, the spectral index of RRATs J0054+66 and J2324-05 were calculated, with the former having a value in the range of 4.6 to 5.3 and is higher than what is expected for regular pulsars. The spectral index of J2324-05 is on the same order as those for regular pulsars, attaining a value between 0.6 and 1.11. Both of these indicate that for those RRATs the LWA can detect, they are much brighter at these low frequencies. While the origin of the RRAT's transient pulsing nature cannot be significantly constrained further by this study, we have demonstrated that RRATs do indeed continue to behave as transients in this little studied frequency band and that some are detectable as regular pulsars for an as yet undetermined amount of time, but later appear to null completely for unknown reasons. Future studies of RRATs with the LWA or other instruments that operate in a similar frequency band and at higher sensitivities will likely provide further clues into RRATs, their emission mechanisms, and their relation to the many other subclasses of pulsars.

References and Acknowledgements

1. Asseo, E. et al. 1990. MNRAS. Volume 247, pp. 529-548
2. Baade, W. et al. 1934. PNAS, Volume 20, 254-259
3. Baade, W. et al. 1934. PNAS, Volume 20, 259-263
4. Bates, S. D. et al. 2013. MNRAS, Volume 431, Issue 2, pp. 1352-1358
5. Bhat, N. D. R. et al. 2003. The Astrophysical Journal, Volume 584, pp. 782-790
6. Bühler, R. et al. 2014. Reports on Progress in Physics, Volume 77, Issue 6
7. Boyles, J. M. et al. 2013. The Astrophysical Journal, Volume 763, Issue 2
8. Burke-Spolaor, S. et al. 2010. MNRAS. Volume 402, Issue 2 pp. 855-866
9. Burke-Spolaor, S. et al. 2011. MNRAS. Volume 416, Issue 4, pp. 2465-2476
10. Burke-Spolaor, S. et al. 2011. The Astrophysical Journal, Volume 727, Issue 1
11. Burke-Spolaor, S. 2013. Proceedings of the International Astronomical Union, Volume 291, pp. 95-100
12. Camilo, F. 1999. Pulsar Timing, General Relativity and the Internal Structure of Neutron Stars. ISBN: 90-6984-247-5
13. Caballero, I. et al. 2012. Memorie della Societa Astronomica Italiana, v.83, p.230
14. Carrol, B. et al. 2006. Introduction to Modern Astrophysics 2nd ed. Addison-Wesley
15. Chen, K. et al. 1992. The Astrophysical Journal, Volume 402, pp. 264-270
16. Cheng, K. S. et al. 2000. The Astrophysical Journal, Volume 537 pp. 964-976
17. Coles, W. A. et al. 2010. The Astrophysical Journal, Volume 717, Issue 2, pp. 1206-1221
18. Condon, J. J. et al. 2010. http://www.cv.nrao.edu/course/astr534/Pulsars.html
19. Cordes, J. M. et al. 2003. The Astrophysical Journal, Volume 596, pp. 1142-1154
20. Cordes, J. M. et al. 2006. The Astrophysical Journal, Volume 637, Issue 1, pp. 446-455
21. Cordes, J. M. 2008. The Astrophysical Journal, Volume 682, Issue 2, pp. 1152-1165
22. Cordes, J. M. et al. 2008. 2002. arXiv: 0207156
23. Cui, B. et al. 2012. arXiv:1210.6002
24. Cui, B. et al. 2015. http://astro.phys.wvu.edu/rratalog/
25. Deneva, J. S. et al. 2009. The Astrophysical Journal, Volume 703, pp. 2259-2274
26. Douchin, F. et al. 2001. Astronomy and Astrophysics, v.380, p.151-167
27. Duncan, R. C. 2003. http://solomon.as.utexas.edu/~duncan/magnetar.html

28. Dykes, J. et al. 2005. The Astrophysical Journal, Volume 626, Issue 1, pp. L45-L47
29. Ellington, S. W. et al. 2013. IEEE Transactions on Antennas and Propagation, vol. 61, issue 5, pp. 2540-2549
30. Karako-Argaman, C. et al. 2015. arXiv:1503.05170
31. Keane, E. F. et al. 2008. MNRAS. Volume 391, Issue 4, pp. 2009-2016
32. Keane, E. F. et al. 2010. MNRAS. Volume 401, Issue 2, pp. 1057-1068
33. Keane, E. F. et al. 2011. Bulletin of the Astronmical Society of India, Vol. 39, No. 3, p. 333-352
34. Gaensler, B. et al. 2007. Astrophysics and Space Science, Volume 308, Issue 1-4, pp. 95-99
35. Ginzburg, V. L et al. 1975. Annual review of astronomy and astrophysics. Volume 13, pp. 511-535
36. Gold, T. 1968. Nature. Volume 218, pp 732, pp. L51-53
37. Hailey, C. J. et al. 2002. The Astrophysical Journal, Volume 578, Issue 2, pp. L133-L136
38. Hernquist, L. 1985. MNRAS. Volume 213, Issue 2. Pp. 313-336
39. Hessels, J. W. T. et al. 2007. 40 YEARS OF PULSARS: Millisecond Pulsars, Magnetars and More. AIP Conference Proceedings, Volume 983, pp. 613-615
40. Hulse, R. A. et al. 1974. The Astrophysical Journal, Volume 195
41. Lattimer, J. M. et al. 2004. Science, Volume 304, Issue 5670, pp. 536-542
42. Levison, A. et al. 2005. The Astrophysical Journal, Volume 631, pp. 456-465
43. Lewandowski, W. et al. 2013. MNRAS. Volume 434, Issue 1, p.69-83
44. Losovsky, Y. et al. 2014. Astronomy Reports, Volume 58, pp. 537-544
45. Lyne, A. et al. 1988. MNRAS. Volume 234, Issue 3, pp. 477-508
46. Lyne, A. et al. 2012. Pulsar Astronomy 4th Ed. Cambridge Press.
47. Manchester, R. N. 1998. Memorie della Società Astronomia Italiana, Vol. 69, p. 801
48. Manchester, R. N. 2001. MNRAS. Volume 328, Issue 1, pp. 17-35
49. McLaughlin, M. A. 2011. AIP Conference Proceedings, Volume 1379, pp. 48-55
50. McLaughlin, M. A. 2009. MNRAS. 400 (3): 1431-1438.
51. McLaughlin, M. A. et al. 2006. Nature, Volume 439, Issue 7078, pp. 817-820
52. Miller, J. J. et al. 2013. The Astrophysical Journal, Volume 776, Issue 2, article id. 104, 9
53. Pacini, F. 1967. Nature, 216, 567-568
54. Perley, R. A. et al. 1984. NRAO Library. http://library.nrao.edu/public/memos/vla/sci/VLAS_146.pdf
55. Rawley, L. A., et al. 1987. Science. vol. 238, pp. 761-765
56. Ruderman, M. A. et al. 1975. Astrophysical Journal, vol. 196, pp. 51-72
57. Sandberg, A. et. 2009. Astronomy and Astrophysics, Volume 504, Issue 2, 2009, pp.525-530
58. Schinzel, F. et al. 2014. http://www.ece.vt.edu/swe/lwa/memo/lwa0202.pdf
59. Shitov, P. Y. et al. 2009. Astronomy Reports V 53, 6. pp. 561-563
60. Stovall, K. et al. 2014. The Astrophysical Journal, Volume 791, Issue 1, article id. 67, 18
61. Taylor, G. B. et al. 2012. Journal of Astronomical Instrumentation, Volume 1, Issue 1
62. Thompson, C. et al. 1993. Astrophysical Journal, Volume 408, Issue 1, pp. 194-217
63. Turbiner, A. V. et al. 2014. Modern Physics Letters A, Volume 19, Issue 25, pp. 1919-1923
64. Verbiest, J. et al. n.d. astronomy.swin.edu.au. http://astronomy.swin.edu.au/pulsar/noteshome/reduction/p2_files/image003.jpg
65. Vivekanand, M. et al. 1982. Journal of Astrophysics and Astronomy, vol. 3, p. 237-247
66. Weisberg, J. M. et al. 2010. The Astrophysical Journal, 722:1030–1034
67. Weltevrede, P. et al. 2006. The Astrophysical Journal, Volume 645, Issue 2, pp. L149-L152
68. Wilson, T. L. et al. 2013. Tools of Radio Astronomy 6th ed. Springer.
69. Wynn, C. G. et al. 2007. MNRAS. Volume 375, Issue 3. pp. 821-830
70. Zhang, B. et al. 2007. MNRAS. Volume 374, Issue 3, pp. 1103-1107
71. Zhang, B. et al. 2005. The Astrophysical Journal, Volume 631, Issue 2

Appendix

Listed below are the python programs and shell scripts used in this study and written by Dr. Kevin Stovall. For more information on the PulsaR Exploration and Search Toolkit (PRESTO) software, please visit http://www.cv.nrao.edu/~sransom/presto/.

plotpulsefromdat.py: This python program plots the time series in the vicinity of a pulse that is given as input.

```python
import matplotlib.pyplot as plt
import sys
import numpy as np
import infodata
import math
import scipy.stats

numpoints=1000
index=sys.argv[1]
indexes=index.split(',')

def rms(num):
    return math.sqrt(float(sum(n*n for n in num))/len(num))

def getpulsewindow(pulseindex,data,cutoff=1.0):
  while data[pulseindex] > cutoff and pulseindex > 0:
    pulseindex=pulseindex-1
  minpulseindex=pulseindex
  pulseindex=pulseindex+1
  while data[pulseindex] > cutoff and pulseindex<len(data):
    pulseindex=pulseindex+1
  maxpulseindex=pulseindex
  return minpulseindex,maxpulseindex

def scatterfit(t,A,taud,beta,phase):
  return np.piecewise(t,[t<phase,t>=phase],[0,lambda t: A*(t-phase)**beta*np.exp(-(t-phase)/taud)])

for filenm in sys.argv[2:]:
  filenmbase = filenm[:filenm.rfind(".dat")]
  info = infodata.infodata(filenmbase+".inf")
  N, dt = int(info.N), info.dt
  data=np.fromfile(filenm, dtype=np.float32, count=N)
  RMS=rms(data)
  data=data/RMS
  for ii,ind in enumerate(indexes):
    index=int(ind)
    signal = data[index-numpoints:index+numpoints]
```

```
  x = np.arange(0.0,numpoints*2,1.0)
  p0 = scipy.array([1.0,10.0,0.4,numpoints])
  print len(x)
  print len(signal)
  try:
    popt, pcov = scipy.optimize.curve_fit(scatterfit, x, signal,p0)
  except RuntimeError:
    popt=[0,0,0,0]
  R=4
  #scatter=scatterfit(x,3.0,100.0,0.4,1000.0)
  #plt.plot(scatter)
  print popt
  pad_size = math.ceil(float(signal.size)/R)*R - signal.size
  b_padded = np.append(signal, np.zeros(pad_size)*np.NaN)-3.0*float(ii)
  newplot=scipy.stats.nanmean(b_padded.reshape(-1,R), axis=1)
 #plt.axvline(x=numpoints/R,ymin=-0.001,ymax=0.002)
  plt.plot(newplot)
 plt.show()
 modelpulse=scatterfit(x,popt[0],popt[1],popt[2],popt[3])
 snr=sum(modelpulse)
 print snr/30.0
 pad_size = math.ceil(float(modelpulse.size)/R)*R - modelpulse.size
 b_padded = np.append(modelpulse, np.zeros(pad_size)*np.NaN)
 newplot=scipy.stats.nanmean(b_padded.reshape(-1,R), axis=1)
 #print newplot
#  plt.plot(newplot)
 beginpulsewindow,endpulsewindow=getpulsewindow(signal.argmax(axis=0),signal)
 beginmodelpulsewindow,endmodelpulsewindow=getpulsewindow(modelpulse.argmax(axis=0),modelpulse,cutoff
=0.1)
 print beginmodelpulsewindow,endmodelpulsewindow
 print "RMS=%f\b" % rms(modelpulse[beginmodelpulsewindow:endmodelpulsewindow])
 print scipy.stats.chisquare(modelpulse[beginmodelpulsewindow:endmodelpulsewindow])
 print scipy.stats.chisquare(signal[beginmodelpulsewindow:endmodelpulsewindow])
 pulsewindow=range(beginpulsewindow,endpulsewindow,1)
 pulsewindowvals=signal[beginpulsewindow:endpulsewindow]
 #plt.plot(pulsewindow,pulsewindowvals,'r-')
 print beginpulsewindow,endpulsewindow
plt.show()
```

crabsearch.py: This program is similar to PRESTO's singlepulsesearch.py, but instead looks for pulses scattered to various extents.

```
import scipy, scipy.signal, scipy.stats
import numpy as np
import matplotlib
#matplotlib.use("macosx")
import matplotlib.pyplot as plt
import sys
import infodata
import math
```

```python
#numpoints=524288
#numpoints=131072
#numpoints=65536
numpoints=32768
#numpoints=16384
#numpoints=8192
statcutoff=4.0
#taud=512
overlap=8192
whichstat=1 #snr=0,snr2=1,chi2=2,mat_cov=3
ploteachpulse=0
def scatter(t,taud=100.0,beta=0.42,phase=0,A=1.0):
beta=abs(beta)
taud=abs(taud)
A=abs(A)
return np.piecewise(t,[t<phase,t>=phase],[0,lambda t: A*(t-phase)**beta*np.exp(-(t-phase)/taud)])
def rms(num):
return math.sqrt(float(sum(n*n for n in num))/len(num))
def prune(candlist):
close = 100
toremove = []
for i in range(len(candlist)):
if candlist[i][3] < close:
toremove.append(i)
toremove = sorted(toremove, reverse=True)
for i in toremove:
del(candlist[i])
return candlist
def prune_related(candlist):
returnlist = []
close = 150
while len(candlist)!=0:
maxindex = argmaxsigma(candlist)
toremove = []
#print candlist[maxindex]
returnlist.append(candlist[maxindex])
for i in range(len(candlist)):
if abs(candlist[i][3]-candlist[maxindex][3])<close:
toremove.append(i)
toremove = sorted(toremove, reverse=True)
for i in toremove:
del(candlist[i])
return returnlist
def getpulsewindow(pulseindex,data,cutoff=1.0):
while data[pulseindex] > cutoff:
if pulseindex>=0:
pulseindex=pulseindex-1
else:
break
minpulseindex=pulseindex
pulseindex=pulseindex+1
while data[pulseindex] > cutoff:
if pulseindex<len(data)-1:
```

```python
        pulseindex=pulseindex+1
    else:
        break
maxpulseindex=pulseindex
return minpulseindex,maxpulseindex
def argmaxsigma(candlist):
maxsigma = 0.0
maxindex = -1
j = 0
for cand in candlist:
    if cand[1] > maxsigma:
        maxsigma = cand[1]
        maxindex = j
    j=j+1
return maxindex
t1 = np.arange(0.0, 4096, 1.0)
t2 = np.arange(0.0, numpoints, 1.0)
searchpulse = []
taud = []
area = []
candlist = []
#for i in range(50,51,50):
# for j in [0.0,0.10,0.20,0.30,0.40,0.50,0.60,0.70,0.80,0.90]:
#for i in [10,20,30,50,100,200]:
for i in [10.0,20.0,30.0,50.0,100.0,200.0]:
    for j in [0.40]:
        searchpulse1 = scatter(t1,i,beta=j)
        searchpulse1 = searchpulse1/np.amax(searchpulse1)
        searchpulse.append(searchpulse1)
        taud.append([i,j])
        areaundercurve=sum(searchpulse1)
        area.append(areaundercurve)
filenm=sys.argv[1]
filenmbase = filenm[:filenm.rfind(".dat")]
signal = np.fromfile(filenm, dtype=np.float32, count=numpoints)
info = infodata.infodata(filenmbase+".inf")
DMs = []
DMstr = "%.4f"%info.DM
DMs.append(info.DM)
DM = info.DM
N, dt = int(info.N), info.dt
obstime = N * dt
outfile = open(filenmbase+'.singlepulse', mode='w')
outfile.write("# DM SNR Time (s) Sample t_d beta\n")
outfile2 = open(filenmbase+'.statistics', mode='w')
outfile.write("# DM SNR SNR2 Red_Chi2 Time (s) Sample t_d beta\n")
data = np.fromfile(filenm, dtype=np.float32, count=N)
startN=0
endN=numpoints
datarms=rms(data)
mean=np.mean(data)
data=data/datarms
datarms=rms(data)
```

```python
while endN<N:
sys.stdout.write("%f\r" % (float(endN)/float(N)))
sys.stdout.flush()
#signal = data[startN:endN]
for j in range(len(searchpulse)):
signal = data[startN:endN]
result = np.correlate(signal,searchpulse[j],mode='valid')
pulseindex = result.argmax(axis=0)
p0 = scipy.array([taud[j][0],taud[j][1],pulseindex,1.0])
#print "Fitting"
try:
popt, pcov = scipy.optimize.curve_fit(scatter, t2, signal,p0)
except RuntimeError:
popt=[1,0,0,0]
if popt[0]==0:
popt[0]=1
#print "Done"
#print popt
modelpulse=scatter(t2,popt[0],popt[1],popt[2],popt[3])
#print "Done"
minpulseindex,maxpulseindex=getpulsewindow(pulseindex,modelpulse,cutoff=0.0001)
snr=sum(modelpulse[minpulseindex:maxpulseindex])/math.sqrt(maxpulseindex-minpulseindex)
snr2=sum(signal[minpulseindex:maxpulseindex])/math.sqrt(maxpulseindex-minpulseindex)
chi2 = sum(((scatter(t2,*popt)-signal)/1.0)**2)
dof = len(signal) - len(popt)
rchi2 = chi2/dof
if whichstat==0:
stat=snr
elif whichstat==1:
stat=snr2
elif whichstat==2:
stat=rchi2
while stat>statcutoff:
b=signal[minpulseindex-50:maxpulseindex+50]
R=4
pad_size = math.ceil(float(b.size)/R)*R - b.size
b_padded = np.append(b, np.zeros(pad_size)*np.NaN)
dataplot=scipy.stats.nanmean(b_padded.reshape(-1,R), axis=1)
times=np.arange(0,len(dataplot),1)
times=(times+startN+minpulseindex-50)*dt
#plt.plot(times,newplot)
b=modelpulse[minpulseindex-50:maxpulseindex+50]
b_padded = np.append(b, np.zeros(pad_size)*np.NaN)
modelplot=scipy.stats.nanmean(b_padded.reshape(-1,R), axis=1)
#plt.plot(times,newplot)
signal=signal-modelpulse
b=signal[minpulseindex-50:maxpulseindex+50]
b_padded = np.append(b, np.zeros(pad_size)*np.NaN)
data2plot=scipy.stats.nanmean(b_padded.reshape(-1,R), axis=1)
#plt.plot(times,newplot)
pulseindex=pulseindex+startN
candlist.append([DM,stat,(pulseindex*dt),pulseindex,popt[0],popt[1],times,dataplot,modelplot,data2plot,snr,snr2,
rchi2])
```

```python
#plt.ylabel("Flux(Arbitrary)")
#plt.xlabel("Time(s)")
#if whichstat==0:
# plt.title("SNR:%f" % stat)
#filename="DM%0.2f_%08d_%0.2fs_snr%0.1f_taud%f_beta%f.png"
(DM,pulseindex,(pulseindex*dt),stat,taud[j][0],taud[j][1])
result = np.correlate(signal,searchpulse[j],mode='valid')
pulseindex = result.argmax(axis=0)
p0 = scipy.array([100.0,0.4,pulseindex,1.0])
#print "Fitting"
try:
popt, pcov = scipy.optimize.curve_fit(scatter, t2, signal,p0)
except RuntimeError:
popt=[0,0,0,0]
if popt[0]==0:
popt[0]=1
#print "Done"
#print popt
modelpulse=scatter(t2,popt[0],popt[1],popt[2],popt[3])
#print "Done"
minpulseindex,maxpulseindex=getpulsewindow(pulseindex,modelpulse,cutoff=0.0001)
snr=sum(modelpulse[minpulseindex:maxpulseindex])/math.sqrt(maxpulseindex-minpulseindex)
snr2=sum(signal[minpulseindex:maxpulseindex])/math.sqrt(maxpulseindex-minpulseindex)
chi2 = sum(((scatter(t2,*popt)-signal)/1.0)**2)
dof = len(signal) - len(popt)
rchi2 = chi2/dof
if whichstat==0:
stat=snr
elif whichstat==1:
stat=snr2
elif whichstat==2:
stat=rchi2
#plt.savefig(filename)
#plt.close()
startN=startN+numpoints-overlap
endN=endN+numpoints-overlap
candlist=prune_related(candlist)
candlist=prune(candlist)
candlist.sort(key=lambda tup: tup[3])
for cand in candlist:
outfile.write("%7.4f %7.3f %13.6f %10d %3d %0.2f\n" % (cand[0],cand[1],cand[2],cand[3],cand[4],cand[5]))
outfile2.write("%7.4f        %7.3f        %7.3f        %7.3f        %13.6f        %10d        %3d        %0.2f\n"        %
(cand[0],cand[10],cand[11],cand[12],cand[2],cand[3],cand[4],cand[5]))
if ploteachpulse!=0:
plt.plot(cand[6],cand[7])
plt.plot(cand[6],cand[8])
plt.plot(cand[6],cand[9])
plt.ylabel("Flux(Arbitrary)")
plt.xlabel("Time(s)")
if whichstat==0:
plt.title("SNR:%f" % stat)
filename="DM%0.2f_%08d_%0.2fs_snr%0.1f.png" % (cand[0],cand[3],cand[2],cand[1])
elif whichstat==1:
```

```
plt.title("SNR2:%f" % stat)
filename="DM%0.2f_%08d_%0.2fs_2snr%0.1f.png" % (cand[0],cand[3],cand[2],cand[1])
plt.savefig(filename)
plt.close()
```

RRATsearch.sh: A script utilized to automate most of the processes required to search a fits file for RRAT candidates.

```
#!/bin/bash
file=$1
numout=`readfile ${file} | grep Spectra | grep file | awk '{print $5}'`
#rfifind -time 10 $file -o ${file:0:${#file}-10} &> ${file:0:${#file}-10}_rfifind.out
for dm in {680..780}
do
mkdir ${file:0:${#file}-10}$dm
newdm=`echo ${dm}/10 | bc -l`
prepsubband -lodm ${newdm} -numdms 100 -dmstep 0.001 -dmprec 3 -nsub 128 -o ${file:0:${#file}-10}$dm/${file:0:${#file}-10} $file -numout ${numout} -mask ${file:0:${#file}-10}_rfifind.mask
cd ${file:0:${#file}-10}$dm
for datfile in `ls *.dat`
do
realfft $datfile
rednoise ${datfile:0:${#datfile}-4}.fft
mv ${datfile:0:${#datfile}-4}_red.fft ${datfile:0:${#datfile}-4}.fft
realfft ${datfile:0:${#datfile}-4}.fft
rm ${datfile:0:${#datfile}-4}.fft
done
/home/kstovall/src/presto_lofreq/bin/single_pulse_search.py -p *.dat
mkdir ${file:0:${#file}-10}$dmscattered
mv ls *.dat ${file:0:${#file}-10}$dmscattered
mv ls *.inf ${file:0:${#file}-10}$dmscattered
cd ${file:0:${#file}-10}$dmscattered
bash wrapper.sh
rm ${file:0:${#file}-10}$dm/*.dat
done
```

fwhm.py: A program that finds the optimum parameters to fit an input pulse to a Gaussian profile.

```
import matplotlib.pyplot as plt
import sys
import numpy as np
import infodata
import math
import scipy.stats
import pylab as plb
from scipy.optimize import curve_fit
from scipy import asarray as ar,exp
numpoints=1000
index=sys.argv[1]
```

```python
indexes=index.split(',')
def rms(num):
return math.sqrt(float(sum(n*n for n in num))/len(num))
def gaus(t,a, sigma,phase):
return (a*math.sqrt(sigma))*exp(-(t-phase)**2/(2*sigma**2))
for filenm in sys.argv[2:]:
filenmbase = filenm[:filenm.rfind(".dat")]
info = infodata.infodata(filenmbase+".inf")
N, dt = int(info.N), info.dt
data=np.fromfile(filenm, dtype=np.float32, count=N)
RMS=rms(data)
data=data/RMS
for ii,ind in enumerate(indexes):
index=int(ind)
signal = data[index-numpoints:index+numpoints]
x = np.arange(0.0,numpoints*2,1.0)
p0 = scipy.array([0.5,0.5,numpoints])
#print len(x)
#print len(signal)
try:
popt, pcov = scipy.optimize.curve_fit(gaus, x, signal,p0)
except RuntimeError:
popt=[0,0,0,0]
print popt
print pcov
```